universität wien

MASTERARBEIT / MASTER'S THESIS

Titel der Masterarbeit / Title of the Master's Thesis

„Does Fronto-Posterior Theta Coherence Predict 6-Months-Old Infants' Orientation Latencies in a Prediction Task?"

verfasst von / submitted by

Matteo Mattersberger, BSc BA

angestrebter akademischer Grad / in partial fulfilment of the requirements for the degree of

Master of Science (MSc)

Wien, 2024 / Vienna 2024

Studienkennzahl lt. Studienblatt / degree programme code as it appears on the student record sheet:	UA 066 840
Studienrichtung lt. Studienblatt / degree programme as it appears on the student record sheet:	Masterstudium Psychologie UG2002
Betreut von / Supervisor:	Univ.-Prof.in Dipl.-Psych.in Dr.in Stefanie Höhl

:

Abstract

Neuronale Theta-Band-Aktivität gilt in der entwicklungspsychologischen Literatur als Korrelat von Lern- und Aufmerksamkeitsprozessen bei Säuglingen und Kleinkindern. Weitere neurowissenschaftliche Befunde aus Studien mit Jugendlichen, Erwachsenen und Tieren, legen nahe, dass Synchronizität im Theta-Band zwischen frontalen und parietalen Hirnregionen einen möglichen Ursprung dieses Zusammenhangs darstellen könnte. Um diese These zu überprüfen, untersuchte die vorliegende Arbeit, ob fronto-parietale EEG-Kohärenz (Magnitude Squared Coherence) bei 6 Monate alten Säuglingen während einer Baseline-Phase einen Prädiktor kürzerer Latenzzeiten zur Orientierung während einer späteren Task-Phase darstellt. Unter Latenzzeiten zur Orientierung wird hierbei die Zeit verstanden, welche ein Säugling benötigt, um seinen Blick auf die durch einen Hinweisreiz vorhergesagte Position eines Zielreizes auf einem Bildschirm zu richten. Die Hypothese dieser Untersuchung war, dass eine höhere fronto-parietale Theta-Band-Kohärenz mit schnellerer Aufmerksamkeitsorientierung, also kürzeren Latenzzeiten, zusammenhängt. Ein solcher Zusammenhang konnte jedoch in der vorliegenden Arbeit nicht nachgewiesen werden.

Contents

Does Fronto-Posterior Theta Coherence Predict 6-Months-Old Infants' Orientation Latencies in a Prediction Task?

In his groundbreaking *Principles of Psychology*, William James (1890/1981) famously characterized infants' sensory experiences "as one great blooming, buzzing confusion" (p. 462). Nevertheless, infants manage to extract meaningful information about their environment from the flow of sensory data available to them, which allows them to increasingly successfully predict, interact with, and navigate their environment over the course of their development. It appears that an intricate interplay of attention allocation and contingency learning is (one of the) key function(s) lying at the heart of this ability (Addyman & Mareschal, 2013; Franchak, 2020; Haith et al., 1988; Johnson et al.,1991; Stahl & Feigenson, 2015).

Despite ongoing efforts and steady improvements in our scientific understanding of early cognitive development, the neural mechanisms underlying this key ability remain poorly understood (cf. Nelson et al., 2012). The subject matter, however, is of relevance beyond the intrinsic value of expanding our scientific understanding of human cognition: Understanding the neural substrate of infant learning processes may prove pivotal in identifying early neural markers of cognitive ability, thus enabling early diagnosis of cognitive atypicalities such as learning disorders, which may in turn allow for providing early intervention and support when needed.

The present thesis aims to contribute to our understanding of the neural mechanisms underlying attention orienting and learning in infants. It aims to examine the hypothesis that synchronicity between frontal and parietal neural populations in the theta band is one of the neural mechanisms underlying these processes in infants. This hypothesis will be assessed by observing whether fronto-parietal coherence in the EEG theta-band during a baseline phase predicts shorter latencies to orient towards a cued target stimulus in a subsequent task phase.

What are the empirical findings justifying the conjecture that fronto-parietal theta connectivity should play the suspected role in infant cognition? The ensuing section will give

an overview of the current literature on the role of theta synchronicity in infant learning and attention and sketch out how it gives rise to the hypothesis under examination.

Theoretical Background

Attention Allocation and Learning

As briefly discussed in the introductory section, infants display an astonishing ability to extract information from and predict stimuli in their environment during the course of their development. Looking behavior plays a crucial role for this ability, as it allows for overtly orienting infants' attention to relevant stimuli (Colombo, 2001). This orientation towards relevant environmental stimuli in turn allows for extracting contingencies in the infant's environment faster, e.g., by allocating their attention so as to avoid redundancies and maximize surprisal (Addyman & Mareschal, 2013; Stahl & Feigenson, 2015). More specifically, it has been suggested that infants focus their attention on external stimuli that maximize their possibility to learn about their environment, thus avoiding completely redundant, as well as completely random (and therefore both non-informative) stimuli (Kidd et al., 2012; Poli et al., 2020). All these findings indicate that the allocation of (visual) attention and the extraction of information about the environment are intimately linked processes in infants, and that the latter is enabled by the purposeful orientation of attention towards informative stimuli which provide learning opportunities.

This type of purposeful orienting towards external stimuli to obtain relevant information is referred to as "visual exploratory behavior" (Franchak, 2020) and becomes more refined over the course of infant development (Colombo, 2001; Johnson et al., 1991). At about one month of age, infants exhibit prolonged fixation on visual stimuli (Johnson, 1990). At about 4 months of age, infants have the ability to make anticipatory eye movements, i.e., direct their gaze towards locations where a stimulus is expected to appear (Haith et al., 1988; Johnson et al., 1991). Haith et al. (1988) found that 3.5 months old participants were able to learn about contingencies in a predictable series of stimuli, which led to shorter latencies to orient towards predicted stimuli as well as to anticipatory looking behavior. They obtained these results by showing 3.5 months old infants two series of stimuli, one predictable (stimuli appear alternating on the left and on the right side with a set interstimulus interval (ISI), and one unpredictable (position and ISI vary randomly), and

observing the effect the predictability had on reaction times and anticipatory eye movements. Similarly, Johnson et al. (1991) found that at the age of 4 months, infants were able to learn the relation between a centrally presented predictor stimulus and a laterally presented target stimulus and to use this knowledge to significantly decrease their mean reaction time to the latter, as well as display anticipatory eye movements. The experimental setup used to arrive at this conclusion consisted of first showing infants one of two moving stimuli ("attractor stimuli") on a central screen. The type of this initial attractor stimulus (type one or type two) predicted the location of a subsequent peripheral stimulus (either left or right side). Using this paradigm, they arrived at the conclusion that the capabilities required for learning environmental contingencies and using this information to reduce reaction times and anticipate external events probably develop between 3 and 4 months of age (at least in their experimental design, although they conjecture based on earlier findings that younger infants may be capable of contingency learning to reduce latencies in simpler tasks).

Thus, the afore characterized combination of attention allocation and learning processes seem to enable infants to react to predicted stimuli in their environment faster and to perform anticipatory eye movements towards the location of expected stimuli.

Neural Correlates of Attention and Learning in Infants

Besides looking behavior, another observable correlate of learning and attention processes in infants is electrophysiological brain activity, as recorded by electroencephalography (henceforth EEG) measurements. EEG is a noninvasive method of measuring neural activity, or – more precisely – the electrical signal generated by it (Wöhrle, 2017). This signal is generated (mostly) by the concurrent excitation of pyramidal cells in the cortex (Bear et al., 2020). To measure it, a set of electrodes is placed on the surface of the scalp, which capture the voltages generated by the firing of large populations of neurons (Bear et al., 2020; Wöhrle, 2017). This measurement will result in a time series of datapoints for each electrode, which can be decomposed into different sinusoidal signals using the process of Fourier transformation, to be explained in more detail in the following

subsections (Cohen, 2014). Repeated synchronous activation of large populations of neurons will result in this activity being observable in the EEG signal in the form of rhythmic waves, which are composed of the aforementioned sinusoidal components (Bear et al., 2020; Cohen, 2014). The most commonly observed types of these waves are categorized according to their frequency and clustered together into distinct kinds: Delta rhythms (<4 Hz), Theta rhythms (~4-7 Hz), Alpha rhythms (~8 -13Hz), Beta rhythms (~ 15-30 Hz), and Gamma rhythms (>30 Hz) (Bear et al., 2020).

There exists a vast and complex array of literature on the functional correlates of these different types of electrophysiological rhythms, from which some reoccurring findings emerge. For the purposes of the present paper, the discussion of these will be limited to the functional correlates of theta-band activity. Activity in this frequency band is reported as playing a role in learning and (working) memory (Colgin, 2013; Liebe et al., 2012; Osipova et al., 2006; Rutishauser et al., 2010; Weiss et al., 2000), as well as in sustained attention (Clayton et al., 2015) and cognitive control (Cavanagh & Frank, 2014; Cooper et al., 2015).

In infants, theta activity corresponds to a different frequency range than in adults, which varies somewhat between authors; the lower end is usually characterized as 2-3 Hertz, and the upper end as 4-6 Hertz (cf. Begus & Bonawitz, 2015; Orekhova et al., 1999; Stroganova et al., 1999). The functional role of these infant theta oscillations is not as well researched as the role of adult theta band activity, but a number of insightful studies exist, which seem to paint a similar picture of theta activity being a neural correlate of cognitive tasks involving attention, learning, and working memory (Begus et al., 2015; Begus & Bonawitz, 2020; Orekhova et al., 1999; Orekhova et al., 2006; Xie et al., 2018). Let us examine some of these results in more detail.

Begus et al. (2015) found that increased theta activity during object exploration was associated with subsequent object recognition in 11 months old infants. In their study, theta power during the exploration of novel object was found to be a significant predictor of an infant's ability to discriminate the object from a similar one in a subsequent comparison (as measured by looking times). Furthermore, several studies indicate a relationship between

electrophysiological theta band activity and sustained (anticipatory) attention (Orekhova et al., 1999; Stroganova et al., 1998; Xie et al., 2018), which consists of maintaining attention while waiting for a stimulus to appear (Xie et al., 2018).

Stroganova et al. (1998) assessed this correlation by comparing theta band activity in 8-11 months old infants during a peek-a-boo game in which a person disappears behind a screen and the infant maintains attention until they reappear to a baseline condition of externally controlled attention (attention to a moving object). They found that theta power increased during the peek-a-boo game compared to a baseline of externally controlled attention (the infant looking at moving objects). This activation was mostly found in frontal areas. These findings led Stroganova et al. (1998) to conclude that this type of frontal theta band activity in infants is likely to reflect frontal executive components of regulating attention.

In a subsequent study, Orekhova et al. (1999) used a similar paradigm to investigate the role of frontal theta in sustained anticipatory attention in infants. They compared EEG activity during externally controlled attention, which was attracted by moving external objects (baseline condition), with EEG activity during sustained anticipatory attention, i.e., the internally controlled attention while awaiting an expected event during a peek-a-boo game. An increase in the theta power spectral density was observed in the test condition compared to the baseline condition, which the authors refer to as “theta synchronization” (Orekhova et al., 1999; also cf. Xie et al, 2018). Furthermore, the authors found that reactivity of frontal theta during sustained attention differentiated between subject’s ability to maintain this type of attention. They concluded that theta synchronization reflected an aspect of cognitive control during the sustenance of attention.

Partially based on these two studies, Xie et al. (2018) also examined the correlation of theta power spectral density and sustained attention in 8 to 12 months old infants using video displays of suddenly disappearing ‘Sesame Street’ characters. Similar to the reports by Orekhova et al. (1999), they found an increase in theta PSD during sustained anticipatory attention in 10- and 12-month-old infants.

In addition to being a correlate of the sustenance and allocation of attention, theta activity has been found to be associated with memory processes in developmental studies. For example, theta band activity is reported to play a role in working memory processes in children (Hermens et al., 2005; Rodriguez-Martinez et al., 2013), though it should be noted that both these studies were conducted among older children and adolescents (6 years and older in Rodriguez-Martinez et al., 2013) or just adolescents (in Hermens et al., 2005). Rodriguez-Martinez et al. (2013) found that spontaneous EEG activity in all frequency ranges, but especially in the theta band, is negatively correlated with working memory capacity. Their interpretation of these findings is that a low level of spontaneous background noise in the theta range facilitates working memory tasks by enabling theta coherence between the involved areas, the idea being that spontaneous activity may interfere with task specific theta activity. This interpretation could account for the results of Hermens et al. (2005), who report that children and adults with ADHD display increased frontal theta activity during a rest condition compared to matched controls.

Furthermore, Braithwaite et al. (2020), as well as Jones et al. (2020), found that infant theta band activity was a significant predictor of cognitive ability in children. More precisely, Braithwaite et al. (2020) found that frontal theta power measured during a non-social baseline video at six months significantly predicted non-verbal cognitive ability at nine months and Jones et al. (2020) found that frontal theta power at 12 months correlated with concurrent cognitive ability and predicted cognitive ability several years later.

To account for findings of the kind reported above, Begus & Bonawitz (2020) propose in a review paper that theta band activity is a neural correlate not only of learning, but of active learning, that is, of being actively cognitively involved during the learning process via the active allocation of attention (Begus & Bonawitz, 2020). Similarly, Bosseler et al. (2013) take theta activity in infants to indicate active control of attention towards informative stimuli during speech perception. This point is succinctly summarized by Begus & Bonawitz (2020) as follows: “Observing an increase in theta activity prior to learning itself strongly

suggests that theta activity is not only involved in incidental learning, but appears to reflect active cognitive engagement" (p. 3).

Although the association of theta with active learning sheds some light on the role of theta-band activity in infant cognition, this correlation alone does suffice as a full-fledged explanatory account. Following common assumptions about the character of scientific explanation in the fields of neuroscience and psychology, such an account would have to specify the causal mechanism giving rise to the correlation (cf. Bechtel, 2008; Craver & Tabery, 2023), i.e., specify its functional role. Before discussing hypotheses and empirical findings regarding the functional role of theta band activity in infants, let us summarize the hitherto discussed key findings pertaining to the role of theta band activity in infants:

Infant theta band activity has been associated with learning and working memory processes in infants. More specifically, it has been hypothesized that theta activity reflects "active learning", that is, the active engagement with and allocation of attention towards stimuli relevant for learning. This is congruent with reports of theta band activity being associated with sustained attention in infants. Theta's functional correlate of attention and learning in infants may be able to account for findings reporting theta band activity being a predictor of cognitive ability later in life.

The Functional Role of Theta Band Connectivity

Some reports suggest that the association between theta activity and cognitive functions such as learning, attention, and working memory is best explained by the theta band's involvement in inter-area communication via neural synchrony (Clayton et al., 2015; Colgin, 2013; Liebe et al., 2012; Rodriguez-Martinez et al., 2013; Weiss et al., 2000). The notion of theta band activity enabling inter-areal communication of neural populations would be in agreement with findings on the role of low-frequency oscillations (such as theta) in distributed brain networks by von Stein and Sarnthein (2000) and Bruns and Eckhorn (2004), who reported that neural networks with greater spatial distribution (i.e., longer range) synchronize at lower frequencies (such as theta), whereas short range networks tend to oscillate at higher frequencies (such as alpha , beta, or gamma). Colgin (2013), proposed

that this may be the case because the coordination between distant brain areas at a lower frequency “permits long synaptic delays and thus can feasibly sustain coupling across distributed brain regions” (Colgin, 2013, p. 306).

While these results pertain to inter-area communication in general, various studies point towards theta synchronization playing this role in networks of attention, learning and memory (Cavanagh & Frank, 2014; Clayton et al., 2015; Cooper et al., 2015; Liebe et al., 2012; Sauseng et al., 2005). For example, Cavanagh and Frank (2014) propose that synchronization in the theta band between frontal and other neural areas is an implementational mechanism for exerting top-down cognitive control in distributed networks. This notion fits with findings by Clayton et al. (2015), who, based on their findings, hypothesize that maintaining sustained attention relies on low frequency synchronization between prefrontal and posterior regions, as well as with reports by Cooper et al. (2015), who found that cognitive control processes were associated with fronto-parietal connectivity in the theta band. The latter was the case both for proactive (i.e., being sensitive to task relevant stimuli) and reactive (i.e., overcoming interference) control processes.

Based on these findings, it seems as though especially fronto-posterior theta connectivity seems to be of central importance for attentional processes. Fitting with the previously established notion of the mechanisms of learning, attention, and memory being tightly linked (at least pertaining to the involvement of theta band activity in these processes), synchronization between frontal and different posterior areas has also been found to be associated with working memory and learning processes:

First, Liebe et al. (2012) report that the strength of theta coupling between area V4 and prefrontal areas was predictive of monkeys’ performance in a visual short term memory task (i.e, stimulus recognition). This, the authors suggest, indicates that theta synchrony is involved in the coordination and cooperation of distant neural ensembles. Second, Weiss et al. (2000) report that in a word recall task, increased coherence in the theta band between anterior and posterior (temporal, parietal, and occipital) areas was associated with the encoding of recalled (as opposed to non-recalled) nouns. Based on their as well as earlier

findings, the authors hypothesize that theta synchrony may be generally associated with demanding tasks requiring efficient information processing. Furthermore, in a study investigating young adolescents, Sauseng et al. (2005) found fronto-parietal theta synchrony (as measured by coherence) to be associated with central executive functions in a working memory task. Similar findings were reported in an older study by Sarnthein et al. (1998), who found that during a working memory task, participants displayed an increased theta coherence between prefrontal and posterior areas both for verbal and visuo-spatial stimuli. Their findings, together with earlier reports, led the authors to conclude that theta synchronization may be a functional correlate of long-range interarea communication, a notion congruent with the explanatory framework laid out at the beginning of the current section. Last, the proposed functional role of theta connectivity as a medium of long-distance inter-area communication would also fit with Rodriguez-Martinez et al.'s (2013) aforementioned proposal, which, to reiterate, stated that a high-level of spontaneous background noise in the theta band may hinder performance in a working memory task by interfering with task-related theta activity. Like Sarnthein et al. (1998), Rodriguez-Martinez et al. (2013) themselves put forth an interpretation of their results in accordance with the framework of theta activity enabling long-distance neural communication, proposing that background theta activity may disrupt this communication process.

Fronto-posterior connectivity playing a key role in processes pertaining to (selective) attention, cognitive control, and working memory fit in with established findings in cognitive neuroscience, namely the theory of the fronto-parietal attention network (Petersen & Posner, 2012; Posner & Petersen, 1990; Posner & Rothbart, 2007). The theory of the fronto-parietal attention network maintains that a distinct interregional network of frontal and parietal regions carries out three distinct functions, namely orientation to sensory events, signal detecting for further (conscious) processing, as well as the maintenance of an alert state (Posner & Petersen, 1990). In the context of the previously discussed cognitive function of selective orientation towards informative stimuli to maximize learning opportunities in infants, it is especially the first of these subsystems which is of interest to the current study.

This “orienting” subsystem is, following Petersen and Posner (2012, p.3) “focused on the ability to prioritize sensory input by selecting a modality or location”, and thus crucial for the ability to allocate attention to informative external stimuli. The orientation subsystem of the attentional system is associated with both frontal and posterior activity (Petersen & Posner, 2012). Corbetta et al. (1998) found orienting responses to be associated with activity in the frontal eye fields (FEF), and Thompson et al. (2005) report the same association in monkeys. Further studies also indicate the involvement of parietal regions in this process: Orienting has been linked to activation of posterior parietal regions in monkeys (Goldberg & Robinson, 1980; Mountcastle, 1978; Wurtz et al., 1980), as well as in humans (Fox & Raichle, 1988) in some (by now) classic studies. The role of the parietal cortex in this network has been hypothesized to be both preparation of motor behavior such as eye movements (Lindner et al., 2010), as well as more “abstract” related processes of attentional allocation (Petersen & Posner, 2012).

To summarize, a large number of studies suggests that fronto-posterior (especially fronto-parietal) theta band connectivity seems to play a key functional role in the allocation of attention, as well as in working memory and learning processes. This fits in with empirical findings regarding large-scale interregional networks communicating via low-frequency oscillations, as well as with the established theoretical body of the fronto-parietal attention system. Furthermore, it can account for the correlation of learning, attention, and working memory processes associated with theta band activity discussed in the previous subsection.

Before discussing how these findings shape the research question underlying the current study, it is worth to explain the hitherto often invoked concepts of “connectivity” and “neural synchrony” at a more comprehensive and technical level. This will be addressed in the following subsection.

Functional Connectivity

Different Types of Connectivity

In the literature on brain connectivity, there exist different (distinct, although partially related) concepts of brain connectivity which ought to be distinguished. First,

anatomical connectivity describes physical connections between remote brain areas by fixed anatomical structures, often via white matter tracts (Lazar, 2010; Zamora-López et al., 2011). This simple neuroanatomical understanding can be distinguished from two other concepts of neural connectivity, namely *effective* connectivity and *functional* connectivity (though, as Fingelkurts et al., 2005, point out, this distinction is at times rather fuzzy, as the formation and elimination of anatomical connections is strongly influenced by executed functions).

Functional connectivity describes statistical interdependencies between different neural populations over time (Friston et al., 1993b). Following Friston et al. (1993b, p. 9), it can thus be defined as "the temporal correlations between spatially remote neurophysiological events". As an inherently correlative measure, functional connectivity does not lend itself easily to causal interpretation (Friston, 1994; Stephan & Friston, 2009). The reason for this is that the direction of influence remains unclear: functional connectivity is incapable of distinguishing between system A exerting an influence on system B, system B exerting an influence on system A, and both system A and B being influenced by system C.

Contrary to the bidirectional measure of functional connectivity, effective connectivity describes asymmetrical relations between neural populations. Friston et al. (1993a, p. 69) define effective connectivity as "the influence one neuronal system exerts over another". Thus, it is capable of specifying the direction of influence and is thus better suited for causal interpretation (Friston, 1994; Stephan & Friston, 2009). Whereas functional connectivity is essentially a correlative measure between two time series, effective connectivity requires more complex model assumptions about the underlying neural system. (Friston, 1994; Stephan & Friston, 2009). It is worth pointing out that the distinction between functional and effective connectivity is better characterized as methodological distinction, rather than a de-re difference between neural mechanisms. That means that the same neural pattern could be characterized as an instance of functional connectivity or as an instance of effective connectivity, depending on the statistical and computational tools used to assess it (Fingelkurts et al., 2005).

Furthermore, although the definition of 'temporal correlations between spatially remote neurophysiological events' suffices as a working definition of functional connectivity, it is important to keep in mind that 'functional connectivity' does not constitute a monolithic concept. As Fingelkurts et al. (2005) emphasize, the concrete conceptualization of functional connectivity, as well as the computational algorithms and metrics used to quantify it, differ between authors. This leads the authors to point out that different measures used to assess functional connectivity do not allow for a simple mapping onto each other, and are not even necessarily directly related, making comparisons between accounts of functional connectivity using differing metrics for quantification somewhat difficult.

Despite these conceptual ambiguities, there have been various efforts to identify suitable measures of functional connectivity, each with their advantages and drawbacks (Bastos & Schoffelen, 2016; Cohen, 2014). These measures include, but are not limited to, spectral coherence (Nunez and Srinivasan, 2006; Shaw, 1984), most commonly calculated as magnitude squared coherence MSC (Schwartz et al., 2017), the imaginary part of coherence ImC (Nolte et al., 2004), the Phase Locking Value PLV (Lachaux et al., 1999), the Phase Lag Index PLI (Stam et al., 2007), and the weighted Phase Lag Index wPLI (Vinck et al., 2001). The following section will go into more detail about the calculation, application, and limitations of spectral coherence, one of the oldest and most widely used of these measures (Miskovic & Keil, 2015).

Coherence

Coherence originated in the fields of mathematics, physics, and engineering (Bendat & Piersol, 1980), and has been used as a standard measure for functional connectivity in neuroscience for several decades (Miskovic & Keil, 2015). It constitutes a measure of the linear relationship between two signals at a given frequency (Nolte et al., 2004). More specifically, it is a measure of phase consistency. As such, it describes the extent to which the differences in phase between two time series signals remain constant over time (Nunez et al., 1997; Nunez & Srinivasan, 2006). Importantly, phase differences between two signals do not by themselves indicate that the signals in question are not synchronized. Assuming even two

Figure 1

Illustration of Synchronized and Asynchronous Signals, Inspired by Cohen (2014)

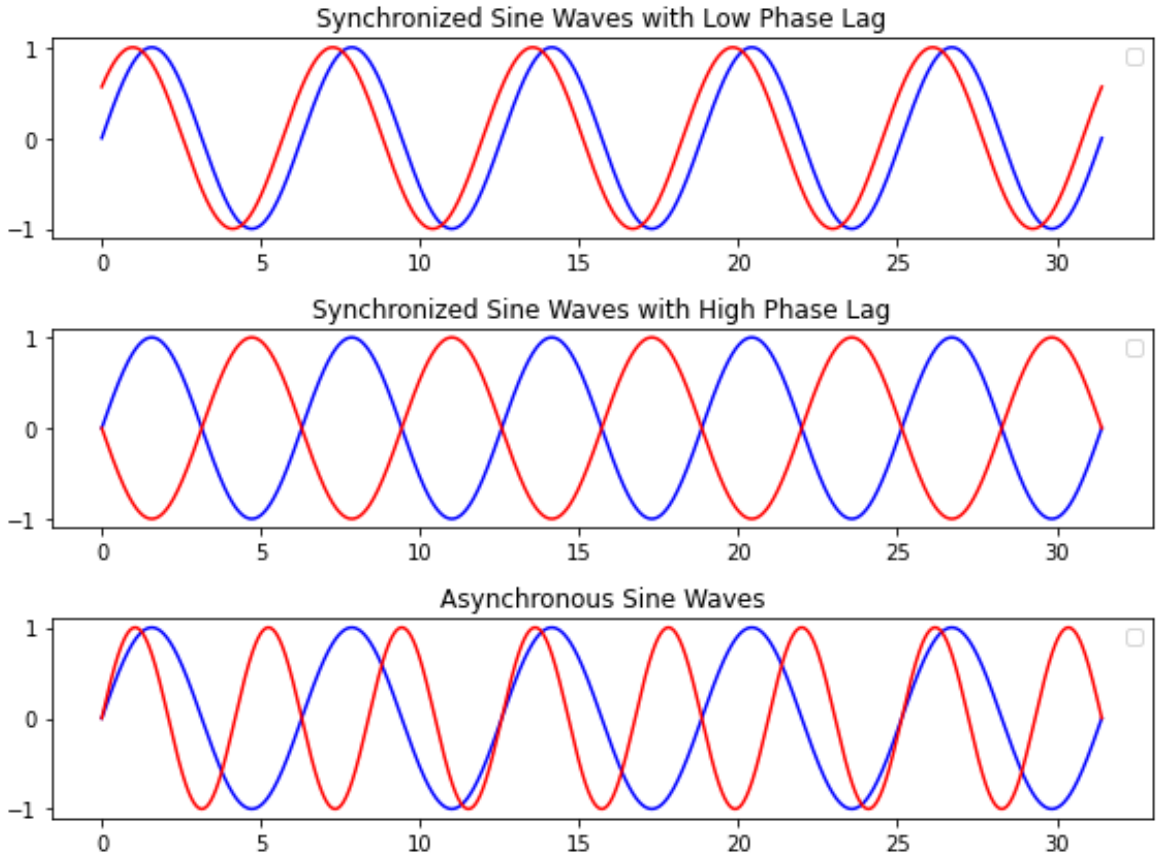

perfectly synchronized neural populations, due to the duration of signal transmission, there will be a phase lag between both cell assemblies. However, given the assumption of synchronization, this phase lag should remain constant over time (Cohen, 2014, see Figure 1 for an illustration). In Figure 1, the sine waves in the first two rows are perfectly synchronized, as the phase lag between both signals in the row remains constant. Contrary to these synchronized signals, the two sine waves in the third row are not synchronized, as the phase lag between them is not constant.

Before delving further into the theoretical and mathematical background of coherence, some conceptual clarifications are in order. 'Coherence' is sometimes taken to be synonymous with 'coherency', e.g., in Nunez et al. (1997) or Nunez and Srinivasan (2006), while the two measures are sometimes also considered to be related but not synonymous measurements, e.g., in Nolte et al. (2004). In contexts where they are differentiated,

'coherency' represents the linear correlation between two sinusoidal signals (such as electrophysiological neural time series data) as a complex number, capturing both amplitude correlation and phase difference (Nolte et al., 2004). On the other hand, 'coherence' specifically denotes the magnitude of this complex representation (Nolte et al., 2004). To understand in detail how coherence (following the latter understanding) between two given time series x and y is computed, it is necessary to first introduce some technical notions, namely that of Fourier transformation, Power Spectral Density (PSD), and Cross Spectral Density (CSD).

The Fourier transformation describes a common procedure in signal processing which transforms a signal representation in the time domain (i.e., a time series) to a representation of the signal in the frequency domain, i.e., a representation of the signal in terms of its constituting frequency components independent of their temporal arrangement (Cohen, 2014; Puschner, 2010). One 'standard' way to apply the Fourier transformation is using the Discrete Fourier Transform (though in practice, more computationally parsimonious methods such as the Cooley-Tukey algorithm are often preferred, cf. Duhamel & Vetterli, 1990), which is computed as follows

$$X_k = \sum_{n=0}^{N-1} x_n * e^{-i\left(\frac{2\pi}{N}\right)kn}$$

with x_n being the data sample at time n, N being the total amount of samples, and k being the frequency index, which indicates for which frequency the Fourier coefficient X is being computed (Cohen, 2014; Puschner, 2010).

The application of the Fourier transformation allows for computing a signal's PSD, which is a measure used in signal processing to analyze the power at different frequencies of a signal (Bizina & Azeez, 2017). It describes how the total power of a signal is distributed over different frequencies (Bizina & Azeez, 2017). Mathematically, the PSD is defined as the Fourier transform of a signal's autocorrelation sequence A, with A being the correlation of a signal x to itself time-shifted by the factor k. Mathematically, A(k) is defined as

$$A(k) = \frac{1}{N} \sum_{n=0}^{N-|k|+1} x(n)x(n+k)$$

with A(k) being the autocorrelation at time lag k, N being the length of the signal, x(n) being the signal at timepoint n, and x(n+k) being the signal at timepoint n shifted by the factor k (Srinivasan, 2007).

Whereas the PSD describes characteristics of only one signal, the CSD function describes the degree of association between the power of two signals at given frequencies. (Srinivasan, 2007). Analogously to the computation of PSD, the CSD is obtained by taking the Fourier transform of the cross correlation of two signals, with the cross-correlation function between two signals as a function of the shift k is defined as

$$T_{xy}(k) = \sum_{n} x(n)y(n+k)$$

with $T_{xy}(k)$ being the cross-correlation as a function of time shift, x and y being the two signals, and n and n+k being the time point under analysis and the time point shifted by k, respectively (Srinivasan, 2007).

Coherence between x and y is then calculated by normalizing the cross spectral density function by the individual power spectral density function (Nunez et al., 1997; Nunez and Srinivasan, 2006). Thus, coherency is calculated as follows:

$$R_{xy}(f) = \frac{P_{xy}(f)}{P_x(f)P_y(f)}$$

with $R_{xy}(f)$ being the coherency between Fourier transforms x and y of two given time series at frequency f, $P_{xy}(f)$ being the cross-spectral density between x and y at frequency f, and $P_x(f)P_x(f)$ being the power spectral densities (or auto spectral density functions) of x and y, respectively (Nolte et al., 2004; Vinck et al., 2001). Coherence, i.e., the magnitude of coherency, is then calculated by taking the absolute value of coherency (Nolte et al., 2004; Vinck et al., 2011):

$$C_{xy}(f) = | R_{xy}(f) |$$

In addition to “coherency” and “coherence”, magnitude squared coherence MSC (which is sometimes used synonymously with “coherence”) is commonly used as an indicator of functional connectivity (Miskovic & Keil, 2015). This value is obtained by squaring the coherence value (Bortel & Sovka, 2006):

$$MSC_{xy}(f) = MSC_{xy}(f)^2$$

For the remainder of this paper, when no further specifications are given, the terms “coherence” and “magnitude squared coherence” will be used interchangeably for the sake of simplicity, as is common in functional connectivity literature (cf. Miskovic & Keil, 2015). It is this latter understanding of coherence (i.e., magnitude squared) that will be referred to by these terms.

Despite being a common measure of functional connectivity, coherence as a measure of neural synchrony is not without problems. Various authors point out two central problems related to the application of coherence in EEG analysis, namely volume conduction and the choice of a reference electrode or electrodes (Lachaux et al., 1999; Nunez et al., 1997; Vinck et al., 2014). Volume conduction denotes the phenomenon that a signal generated by a single cortical source can be detected by multiple scalp electrodes (Cohen, 2014). Within functional connectivity analysis, this poses challenges, as it can yield spurious synchrony. This perceived phase locking may, in reality, arise from the same signal being registered by both electrodes under examination (Cohen et al., 2014; Lachaux et al., 1999).

A common strategy to mitigate the impact of volume conduction involves “referencing” the signals, which involves subtracting a reference signal from the time series under analysis (Nunez and Srinivasan, 2006). This reference can be either an additional electrode or the average signal derived from all recorded electrodes. The rationale behind this procedure is to diminish or neutralize the shared activity detected by multiple electrodes, thus ensuring the resulting signals more accurately reflect localized activity and reducing the influence of spurious synchronicities induced by volume conduction (Cohen et al., 2014; Nunez et al., 1997; Nunez and Srinivasan, 2006).

This leads directly to the second (and more practical) central problem alluded to previously, namely, the choice of an adequate reference electrode (or electrodes). Nunez et al. (1997) delve into the choice of the reference electrodes extensively but do not arrive at a definitive conclusion or recommendation. They emphasize that without a comprehensive volume conductor model and prior knowledge of the location of the signal's cortical sources, it becomes unfeasible to evaluate the impact of a reference on functional connectivity metrics. However, in a subsequent publication, Nunez and Srinivasan (2006) point out that, despite certain shortcomings, the strategy of average referencing can be a good choice when one is interested in reference-independent potentials (i.e., measuring potentials which are not valid only with respect to one particular reference location).

To summarize, functional connectivity describes the statistical interdependencies between two neural populations over time. A commonly used measure of functional connectivity is coherence, which is usually calculated as the magnitude-squared coherence value. This value describes the phase consistency of two oscillatory signals at a given frequency. To avoid the problem of volume conduction, referencing the time series data is standard procedure. Although different choices for adequate reference data exist, a commonly used strategy is referencing the data to the channel average time series. Having thus established the theoretical background of the present paper, let us examine how it relates to the study at hand.

Current Study

Section 1.1 discussed infants' intentional allocation of attention towards informative stimuli to produce learning opportunities. The ability to thus extract information from their environment has been associated with infants' ability to reduce reaction times to predicted stimuli and perform anticipatory eye movements. Section 1.2 introduced the notion of these processes of learning and attention being correlated with infant theta band activity. A possible neural mechanism for this correlation was discussed in section 1.3, namely, theta band connectivity between frontal and parietal regions in a distributed attention network.

Section 1.4 further elucidated the notion of functional connectivity and introduced the notion of spectral coherence as a common measure of it.

Based on these theoretical foundations and empirical findings, the present study aims to investigate whether functional connectivity in the theta band (as measured with coherence) between posterior and frontal areas while watching a video of nonsocial stimuli predicts shorter orientation latencies in a learning/prediction task. The underlying assumption is that an increased theta band coherence between these areas will be associated with an increased ability to maintain attention and orient towards informative stimuli, thus allowing the infants to learn the association between predictive and predicted stimuli faster, and therefore lead to shorter orientation latencies towards the predicted stimuli.

In addition to this main analysis, the data collected during the tasks described in the subsequent sections have been analyzed and presented during a poster presentation (Ruess et al., 2023). Although these analyses will – due to their different aims, methods, and theoretical background – not be discussed in the main body of the present thesis, the contents of the presented poster can be found (formatted but otherwise left unchanged) in Appendix IV.

Materials and Methods

Participants

One hundred forty approximately 6-month-old infants participated in the study. Participants were recruited by contacting caregivers who had previously consented to be included in the university's database and whose children matched the desired age criteria of 6 months. 76 female (mean age = 199.8 days) and 64 male infants (mean age = 198.7 days) participated in the study

Study Design

The experiment comprised three parts, during all of which EEG activity and eye movements (via video recordings of the infant during the tasks) were recorded. First, infants were shown a baseline video displaying non-social, moving objects, such as an airplane, a toy train, moving geometric shapes, etc. (for illustration of example stimuli, see Figure 2). All the displayed objects were 3D animations, rather than real video recordings. The used baseline video had previously been used by Braithwaite et al. (2020) and Jones et al. (2020), and is accessible using the following link: https://bit.ly/3N5KGNW

After the baseline video, the participants completed a gaze cue task, which is not analyzed for the main research question (but is analyzed in the poster found in Appendix IV). The second task following the baseline video was a prediction task (consisting of 48 total trials), which started with a fixation cue with a duration randomized between 500ms and 750ms. Said fixation cue was followed by a picture of a centrally gazing (as if looking at the participant) female face. Laterally at both sides towards the edge of the screen, two identical non-social stimuli were presented at the same time as the face. Both objects were flickering at different frequencies, either both within the infant theta band (“theta trials”, objects were flickering at 3.43 Hz and 4.5 Hz), both within the infant alpha band (“alpha trials”, with objects flickering at 5.54 Hz and 6.55 Hz) or one within each frequency range (“mixed trials”, with objects flickering at 4.5 Hz and 6.55 Hz). There were 16 trials for each trial type. After two seconds, the centrally gazing face as well as the two flickering objects disappeared and a ‘reward stimulus’ appeared in place of one of the two flickering objects (i.e., either at the right or the

Figure 2

Frames From the Baseline Video

left side of the screen. The reward stimulus consisted of a moving cartoon character accompanied by a sound. The location of said stimulus was predicted by the flickering rate of the lateral objects, with either the higher or the lower frequency predicting the reward position (counterbalanced between participants, i.e., for any given participant, either the higher or the lower frequency was predictive of the position of the reward throughout all trials). For an illustration of the task design, see Figure 3. The order of the trials was randomized, with the only constraint being that there cannot be more than three “alpha” or “theta” trials in a row.

Procedure

Data collection was carried out at the Wiener Kinderstudien laboratory at the Department of Developmental and Educational Psychology at the University of Vienna. Upon their arrival, infants and their caregivers were greeted by university staff and led to the

Figure 3

Stimuli Displayed in Prediction Task

Note. The figure illustrates the sequence of stimuli displayed during the prediction task (from left to right). Displayed is a mixed trial (4.5 Hz and 6.55 Hz) with the higher frequency (on the right-hand side) being predictive of the reward stimulus.

laboratory. Before conducting the experiment, the experimental procedure was explained, and potential open questions addressed. Written consent to participate in the study, as well as for the produced video material to be analyzed, was given by the caregivers. Furthermore, they were informed that pauses could be requested at any time, as well as that the experiment could be discontinued without a specification of reasons. The head circumference of the infant was measured, and an EEG cap of the adequate size prepared by another university staff member during the debriefing.

Afterwards, caregivers and infants were led to the experimental site, where the prepared EEG cap was put on. After taking a photograph of the infant and caregiver for the certificate of participation, impedances were tested and – if necessary - improved by applying more EEG gel. If wearing an EEG cap was not possible, the experiment was continued without the recording of electrophysiological data.

After the equipment was set up and the impedances sufficiently low, the participants and the computer screen displaying the experimental stimuli were secluded from the rest of

the laboratory with a dark curtain. Then, the experimental stimuli (as described in the previous subsection) were displayed on the screen. If necessary (either because of the caregiver's wishes or due to the behavior of the infant), the experimental procedure was paused until it was possible to continue testing. If the latter was not possible, parts of the experimental procedure could be skipped, or the testing discontinued.

After the experiment, infants and caregivers were offered a present (infant toy of their choice), a certificate of participation was presented, and a compensation for travelling expenses (six Euros) paid.

Materials

The experiments were conducted in a darkened EEG laboratory, in which a section dedicated to the display of the experimental stimuli was partitioned off by a dark curtain. Two cameras were positioned within this designated area, one above the testing screen, capturing frontal views of the participants (enabling subsequent eye-movement analysis), and another laterally behind the participants, recording both their rear and the testing screen. The software VideoSyncPro (version 2.5.7.5) was used to record and store the video files. The participants viewed the experimental materials on an iiyama G-MASTER GB2560HSU screen with a refresh rate of 144Hz.

For EEG recordings, an infant sized Easycap 32channel actiCAP snap with pre-applied EEG gel and a BrainProducts BrainAmp DC amplifier system was used, and the signal was recorded by the program Brain Vision Recorder (version 1.24.0001). The EEG signal was sampled at a rate of 500 Hz, and impedances were kept below <10 kΩ whenever possible.

Measures

Orientation Latencies

To obtain the mean orientation latencies for each participant, the video recordings of the experimental sessions were manually assigned codes corresponding to the displayed looking behavior using Mangold Interact. After synchronization of the videos with EEG event markers was ensured or - if necessary - adjusted, the behavior of the infants during the tasks

was coded as “looking center”, “looking left”, “looking right”, “not looking”, “distracted”, and “not codable”, and as “looking” or “not looking” during the baseline video.

After coding, data files containing looking behavior codes were exported as .csv files and orientation latencies then calculated using a custom script (written in Python, version 3.8.10), which first selects all trials during which the infant looks towards the center of the screen during the reward onset, and then calculates the difference between the onset of the reward stimulus and the time of gaze orientation towards the stimulus. However, for the latency between stimulus appearance and gaze orientation to be included in the final average value calculation, two conditions ensuring the validity of the trial must be fulfilled: First, the orientation towards the location of the reward must occur before the onset of the fixation cue marking the end of the trial. Second, trials are valid only if no other looking behavior is displayed between the central gaze and the orientation towards the location of the reward, i.e., if the stimulus appears laterally on the left-hand side, but the infant first looks right and then orients towards the stimulus, then the trial is considered invalid and not used for the mean calculation. In order to ensure that reaction times reflect actual responses to the experimental stimuli rather than spurious movements (and thus data noise), trials with reaction times lower than 100ms were excluded from the analysis. This criterion aligns with the threshold used by Matsuzawa and Shimojo (1997), who studied orientation latencies to peripheral stimuli in infants (2.5-12 months), thus providing a methodological precedent applicable to the current study. The remaining trials were then used to calculate the overall mean orientation latencies, as well as the mean orientation latencies for each trial type (alpha, theta, mixed-alpha, mixed-theta). The full analysis script can be found in Appendix subsection 8.1.

Mean Theta Coherence

Before preprocessing the electrophysiological recordings, the segments of the EEG time series corresponding to the baseline-video phase of the experiment were extracted and stored separately. All subsequent preprocessing and analysis steps were performed on these baseline-only datafiles to ensure that no datasets were needlessly excluded. The latter could

be the case if compromised quality of the EEG data during the experimental task led to the entire dataset missing the participant inclusion quality criteria (specified later in section 3.5.3), e.g. due to issues with one or more channels of interest emerging only halfway through the experiment.

Data preprocessing was performed using the HAPPILEE v4 automated preprocessing pipeline for MATLAB, which is suitable for low density (i.e., 32 channels or fewer) EEG data (Lopez et al., 2022). All subsequently described preprocessing steps were carried out using HAPPILEE v4.

First, line noise reduction was implemented using EEGLAB's CleanLine plugin (Mullen, 2012), which employs multi-taper regression to remove suspected line noise from the EEG signal (Lopez et al., 2022). A bandpass filter with a lowpass cutoff of 40 Hz and a highpass cutoff of 1 Hz was then implemented. After the data was filtered, bad channels were automatically detected using EEGLAB's Clean Rawdata function (Kothe & Makeig, 2013) by applying the 'Line Noise Ratio Criterion' set to 2.5 standard deviations (and marking channels which exceed this threshold as bad) and the "Channel Correlation Criterion', which marks channels with a correlation to an already rejected channel exceeding .7 as bad (Lopez et al., 2022), followed by a final spectrum-based detection step (Lopez et al., 2022). This procedure aims to ensure the removal of electrodes with excessively high impedances, damaged electrodes, a lack of scalp contact, or an excessively high rate of movement or electromyographic (EMG) artifact in the data from further processing. In order to achieve artifact removal without the loss of any timepoints in the data, wavelet thresholding was implemented in a subsequent step (Lopez et al., 2022). This processing step was performed by first wavelet transforming the signals of each channel, thus resolving them into their component frequencies, thresholding the transformed data to isolate artifact components by assessing their deviance from the rest of the signal, and finally applying the inverse wavelet transform to obtain an artifact time series (a time series containing only the data identified as noise) from the thresholded wavelet coefficients, which is then subtracted from the original time series, therefore removing the suspected artifacts (Lopez et al., 2022). After

wavelet thresholding, the data was segmented into one second epochs (as recommended by Haartsen, 2019) and previously identified unusable channels were interpolated based on existing channel data (using spherical interpolation, Lopez et al., 2022). Segment rejection was not applied during preprocessing, as the preprocessing procedure was already sufficiently extensive to – in conjunction with the data inclusion criteria specified in the subsequent subsection – ensure the quality of the analyzed data. However, segment rejection based on the infant's looking behavior was implemented in the custom analysis script, as will be explained in the following paragraphs. Last, the data was re-referenced to the average of all channels (see the introductory section for a theoretical justification of this choice; cf. also Nunez and Srinivasan, 2006). The specific input parameters chosen for the execution of the HAPPILEE v4 pipeline can be found in Appendix II subsection 8.2. The specific exclusion criteria based on the afore described preprocessing steps are described in detail in section 3.5.

In the next step, the mean infant theta (3-5 Hz) coherence (defined as magnitude squared coherence) between frontal and parietal regions was calculated. Following the precedent set by previous literature (Gou et al., 2011; Perone et al., 2018; Perone & Gartstein, 2019; Tomalski et al., 2013), which was adjusted to the channels available for the analysis, "frontal areas" were defined as channels F3, F4, Fz, and "parietal areas" were defined as channels P3, P4, and Pz (see Figure 4 for an illustration). The computational procedure was as follows: First, the data files were loaded into the MATLAB toolbox EEGLAB (version 2023.1), a toolbox specialized for EEG data analysis (Delorme & Makeig, 2004). Then, relevant epochs, that is, epochs between the onset and offset marker of the baseline video which were coded as "looking onscreen" during the manual video coding, were selected. Thus, only EEG data which was recorded while the infants were looking onscreen during the baseline video was processed. Once relevant data segments were isolated, the mean fronto-parietal theta (3-5 Hz) coherence for each segment was calculated and the segment scores averaged to obtain a single coherence score for each participant (as recommended by Lachaux et al., 1999 and Nunez et al., 1997, and following the precedent of Meijer et al., 2014

and Nolte et al., 2004). To this end, the magnitude-squared coherence in the infant theta frequency band for each individual epoch was computed between all 9 channel pairs across the two regions of interest (following the precedent of Perone & Gartstein, 2019), thus resulting in 9 inter-ROI coherence scores. This processing step was implemented using the MATLAB function "mscohere()", which relies on the application of Welch's (1967) averaged modified periodogram method (Mathworks, 2023). The 9 scores thus obtained were then averaged within each epoch, resulting in a single mean coherence score per epoch (see Figure 5 for an illustration). Last, these individual epoch values were averaged over the time series to obtain a single coherence value per participant. The script containing the exact computational steps employed can be found in Appendix II subsection 8.3.

Data Preparation & Exclusion Criteria

Included in the final analyses were available participants with both an available mean baseline coherence value satisfying the applied EEG quality criteria (specified below) as well as an available mean orientation latencies value based on at least three trials, neither of which lies outside the lower and upper bound of the interquartile range (IQR) * 1.5 for the respective variable.

Out of the 140 initial datasets, 3 were missing the event markers necessary for selecting the baseline time series and perform the subsequent analyses and were thus excluded. The following inclusion criteria were then applied for the remaining EEG datasets based on the data quality and pipeline quality reports generated as part of the HAPPILEE preprocessing pipelines, following recommendations of the HAPPE user guide (Monachino et al., 2023). The first criterion for inclusion was the r Pre/Post Wavelet Thresholding Value being >0.1, as recommended by Monachino et al. (2022). Assessed were only frequencies below 10 Hz and above 2 Hz, as this is the frequency range in which the spectrum of interest (infant theta, 3-5 Hz) lies. The application of this quality assessment criterion led to the exclusion of 16 participants. The second inclusion criterion was a sufficient number of non-interpolated channels. Participants with fewer than 2 non-interpolated channels per region of interest (i.e., fewer than two channels in either the frontal or the parietal channels of

interest) were rejected from further analysis, again following recommendations of the HAPPE user guide (Monachino et al., 2023). This exclusion criterion led to the further exclusion of 9 datasets. In accordance with recommendations by the HAPPE userguide (Monachino et al., 2023), the further criteria of sufficient length of the datasets and a sufficiently high r Pre/Post Line-Noise Removal value (close to 1, cutoff was set at 0.9 for the Frequencies surrounding the frequency of linenoise, i.e., 50 Hz) were applied. However, these criteria did not lead to the exclusion of any participants who remained in the sample after the application of the first two criteria. Therefore, after performing dataset exclusion based on data quality and pipeline quality assessments, the number of remaining usable datasets was 112.

It was then assessed for how many of these 112 datasets corresponding mean orientation latencies values were available. The inability to obtain a mean orientation latency value could be due to one of four reasons. First, due to missing triggers in the respective looking behavior data files, which were necessary for the computations executed on them. Second, due to a lack of valid trials, that is, a lack of trials in which the infant did look towards the screen during the onset of the reward stimulus and then subsequently moved their gaze towards the stimulus location before the end of the trial in at least three trials. Third, due to altogether missing looking behavior data. Last, 6 values were not obtainable due to errors of unknown origin, possibly due to corrupt datafiles. A lack of usable mean latencies values led to a further dropout of 22 participants, leaving 90 usable datasets.

Before conducting further analyses, statistical outliers were removed using inter-quartile range (IQR), with the lower and upper bound of the datasets set to 1.5*IQR, following convention (Yang et al., 2019). This criterion was applied to both variables under consideration. One participant whose mean baseline theta coherence or mean orientation latencies were outside these cutoffs was removed from further analysis. Thus, the final n for the analyses to follow was 89.

Figure 4

Region of Interest (ROI) Specification Used in Coherence Analysis

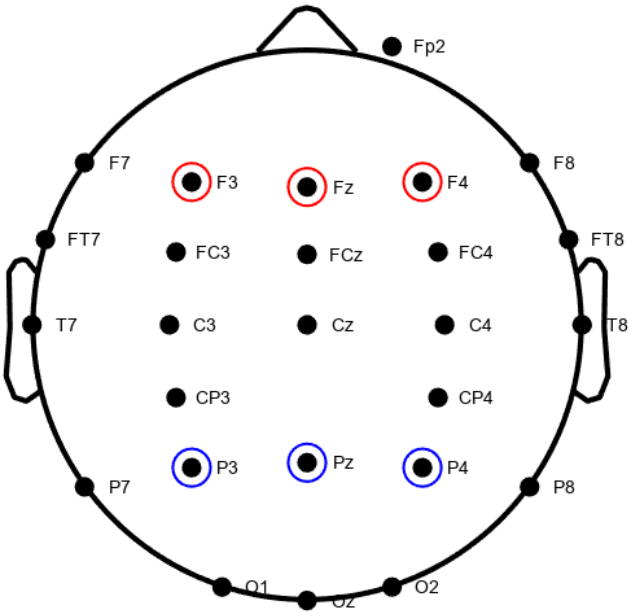

Note. Frontal areas (marked red) were defined as channels F3, Fz, and F4. Parietal regions (marked blue) were defined as regions P3, Pz, and P4. Not all 32 channels are shown in the illustration.

Figure 5

Calculation of Inter-ROI Mean Magnitude Squared Coherence for Epoch n

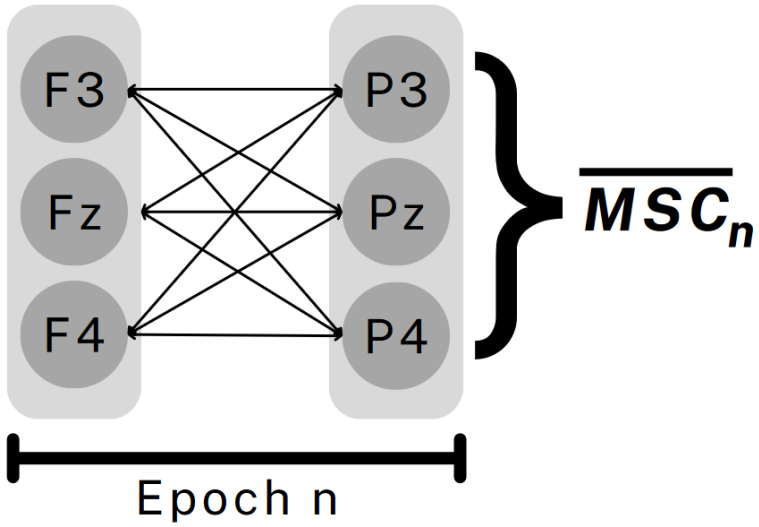

*Note F*or any given epoch n, a matrix containing the MSC values for all possible pairings of electrodes in region of interest (ROI) 1 and region of interest (ROI) 2 was calculated. This matrix was then averaged, to obtain a mean magnitude squared coherence score ($\overline{MSC}$) for n.

Statistical Analyses

A Bayesian Linear Regression Analysis (n=89) was implemented using JASP (JASP Team, 2023) to determine whether a participant's mean coherence during the baseline video predicted their mean orientation latencies during the prediction task. As per JASP's default settings, the parameters chosen for the analysis were as follows:

For the regression coefficients, a Jeffreys-Zellner-Siow (JZS) prior was selected, which combines a Cauchy distribution (a t-distribution with one degree of freedom, Rouder et al., 2009) as the prior for the slope coefficient β (de Vries & Morey, 2013) with a Jeffreys prior, which is a very broad, non-informative prior on the error variability, and a standard choice in Bayesian data analysis (Jeffreys, 1961; Rouder et al., 2009). The Cauchy distribution is 'heavy-tailed', implying that while slope values near zero are most likely, large effects are not precluded, although they get progressively less probable the larger they become (de Vries & Morey, 2013). The exact prior probability distribution for different β-values is determined by the scaling parameter r, which denotes half the inter-quartile range (IQR) of the distribution (so that $r = {}^{IQR}/_{2}$), and thus corresponds to the "flatness" of the distribution's tail (de Vries & Morey, 2013). A smaller r leads to a narrower distribution, representing a stronger prior belief in no or only small effect, whereas a larger r indicates a prior belief in a greater range of plausible effect sizes, reflecting less prior certainty (Heo & Van der Schoot, 2020). For the current study, the Cauchy distribution's scaling factor was set to r=0.354, thus striking a compromise between a prior belief too narrowly focused on small or no effects and a prior belief allowing for implausibly large effects (thus again following JASP's default settings, JASP Team, 2023). For an illustration of the scaling parameter r on distribution properties, see Figure 6 in Appendix I.

For model comparison, the model prior was specified as a Beta Binomial distribution (a=1; b=1), thus assuming a uniform prior probability of both (null and alternative) models. This entails that in the model comparison, no a priori preference will be given to either the null model or the alternative model. The latter may be a valid approach if there are strong reasons for suspecting either of these two models to represent the relation between predictor

and criterion more accurately. However, as described above, no such prior assumptions were made for the present analysis.

Last, for assessing the numerical accuracy, 1000 samples were drawn from the posterior distribution of the regression coefficients and used to compute the 95% credible intervals for the regression coefficients. These credible intervals specify the range of values in which the parameters lie with a 95% probability given the prior assumptions and the observed data (cf. Lu et al., 2012).

After the computation of the posterior models, several model assumption checks were performed to assess the suitability of the data and the validity of the resulting models, following recommendations by van den Bergh et al. (2021). First, a visual assessment of the scatter plot of the predictor against the criterion was performed to identify potential nonlinear trends in their relationship (see Fig. 7). No such trends were identified using visual assessment. Second, the normality of the regression model residuals was assessed using a Q-Q plot (see Figure 8 in Appendix I). If the normality assumption for the model residual holds, all points on the plot should approximately form a straight line. Visual inspection of the Q-Q plot indicates that this assumption holds. Last, homoscedasticity of the data was assessed using a plot of the residuals against the predicted values (see Fig. 9 in Appendix I). A strong curvature of the plot away from the center line would indicate a violation of modelling assumptions regarding homoscedasticity, which in turn may indicate non-linearity in the predictor-criterion relation (cf. Mansfield & Conerly, 1987; van den Berg et al., 2021). Although the plot largely followed the trajectory of the center line, a slight curvature could be observed towards the edges of the data cloud.

Although the trend away from the centerline was not grave, to address the issue of potential non-linearity, two additional models were fitted to the data using a custom script written in Python (version 3.8.10), using the PyMC (version 5.7.2) and ArviZ (version 0.15.1) libraries. These models consisted in second and third order polynomials being fitted to the dataset using Bayesian regression modelling. The reasoning behind this procedure is that – should a non-linear relation hold between the criterion and predictor variable - these more

complex non-linear models should outperform the simpler linear model regression model, as they can adequately capture these non-linearities in the criterion-predictor relation. Subsequent model comparison employing two common criteria in machine learning model selection (Widely Applicable Information Criterion (WAIC) and Leave-One-Out Cross Validation (LOO)) indicated a superior model performance of the linear model compared to the non-linear polynomials. Both WAIC and LOO are measures for assessing out-of-sample prediction accuracy in Bayesian models which aim to punish unnecessary complexity in models to prevent overfitting and thus provide useful guidelines for Bayesian model selection (Vehtari et al., 2017). The linear model had a LOO score (rounded to three digits) of -128.045 and a WAIC of -128.04, the second order model had a LOO value of -128.416 and a WAIC of -128.38, and the third order model had a LOO score of -129.037 and a WAIC of -128.98. Both for WAIC and for LOO, values closer to zero are preferable. Thus, the resulting values indicate that the more complex higher-order regression models did not outperform the simpler linear model, thus validating the model choice employed in the main analysis. The custom script used for model fitting can be found in Appendix II. The exact choice of model prior selection and a detailed breakdown of the models can be found in Appendix III.

In summary, the visual inspection of the aforementioned plots in conjunction with the fitting and comparison of polynomial models indicated no non-linearities or other assumption violations in the predictor-criterion relation, thus making Bayesian linear regression a suitable analysis method for the data at hand.

Figure 7

Mean Fronto-Parietal Theta Coherence Plotted Against Mean Orientation Latencies (in ms)

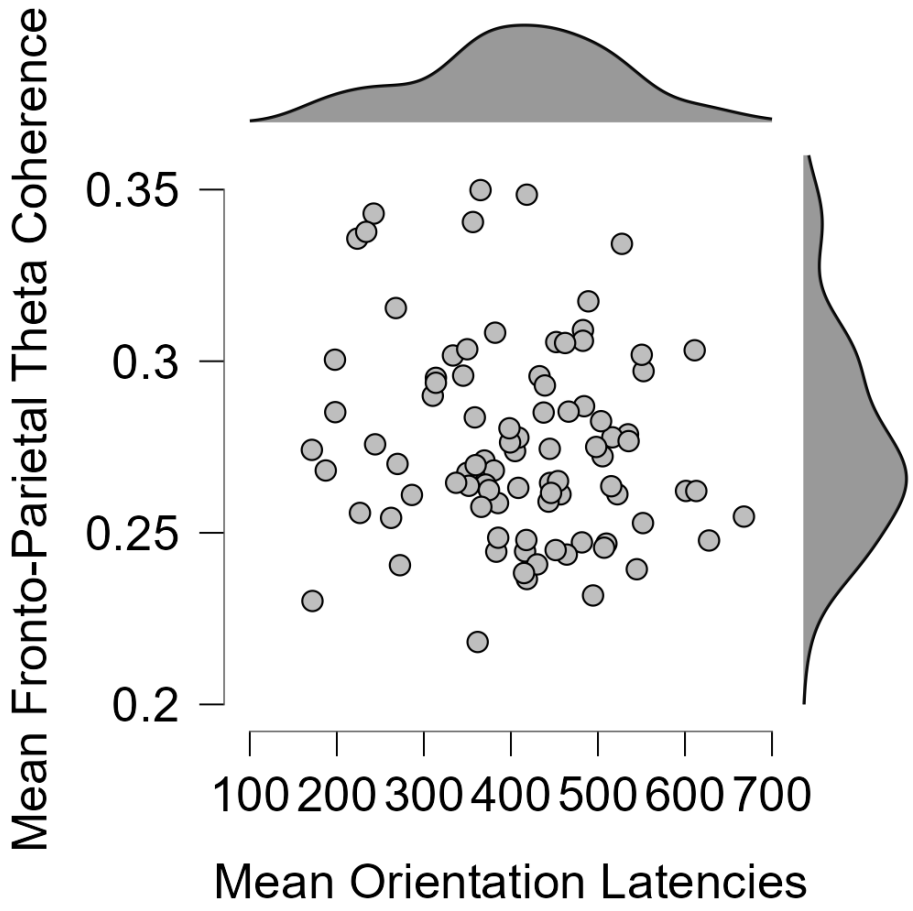

Note Upon visual inspection, the relationship between both variables displays no nonlinearities, such as curvilinear trends in the data cloud (s-shape, u-shape, etc.).

Results

Descriptive Analytics

For the analyzed sample of 89 participants, the mean fronto-parietal theta band coherence was 0.276, with an SD of 0.029 (minimum = 0.218, maximum = 0.350). The distribution of this property had a skewness of 0.680 and a kurtosis of 0.144. The magnitude of the observed coherence values seems plausible in the light of earlier infant coherence studies. For example, Cuevas and Bell (2011) found fronto-posterior baseline coherence in the 6-9 Hz frequency range to be ranging from 0.2 to 0.35, depending on the specific age of the participants (between 5-10 months of age) and electrode pairs analyzed. Similar results were obtained by Bell and Wolfe (2007), who found fronto-parietal coherence in the 6-9 Hz frequency in infants during a baseline phase to be – on average – around 0.3. Furthermore, Meijer et al. (2014) found the mean theta coherence between various scalp electrodes (averaged over multiple ~2.5-hour recording, including waking and sleeping phases) in preterm newborn infants to be between ~1.5 and ~2.5. Although none of these previous findings exactly match the parameters of the present study (age, frequency band, regions of interest, circumstance of data collection), all of them significantly overlap in regard to at least some of these properties, making them relevant precedent for the current study. In light of these earlier findings, the coherence values obtained in the present study seem to be within plausible bounds, and do not give reason to suspect substantial contamination of the results by artifacts.

The mean latency to orient was 408.995ms, with an SD of 110.531ms (minimum = 171.333, maximum = 667.733). The distribution displayed a skewness of -0.181 and kurtosis of -0.284. See Figures 10 and 11 for an illustration of the distribution of both mean coherence and mean latencies values.

Model Posterior

The posterior distribution of the null model including only the intercept as a predictor yielded a mean of 408.995 for the intercept with a standard deviation (SD) of 11.697, and a 95% credible interval (CI) ranging from 385.965 to 431.505. In the posterior

distribution of the alternative model, which includes “fronto-parietal theta coherence” as a linear predictor, the mean of the posterior distribution for the slope was -491.354 (standardized regression coefficient (cf. Siegel, 2016) β = -0.129), with an SD of 381.620, and a 95% CI from –1059.310 (β = -0.278) to 47.810 (β = 0.013). This means that in light of the observed data, the distribution of the most probable slope parameter shifted from a mean of 0 (the prior assumption specified in the previous section) to a posterior distribution with the mean of the slope being -491.354. Repeated sampling of this distribution (also specified in the previous section) yielded the credible interval of the slope parameter specified above, which means that, given the data and the prior assumptions, there is a 95% probability of the slope parameter being in this range. Albeit mathematically differently derived, this interval is comparable in practice to frequentist confidence intervals (cf. Lu et al., 2012).

The posterior distribution of the regression parameters is illustrated in Figure 10[1]. For an illustration of the null model and its 95% credible interval, see Figure 12. For an illustration of the alternative model and its 95% credible interval, see Figure 13.

Model Comparison

The subsequent Bayesian model comparison compared the alternative model (which includes mean fronto-parietal theta coherence as a predictor for orientation latencies) to an intercept only model (the null model), both described in the previous section. This model selection resulted in a posterior probability of the null model (intercept only) of 0.664 and a

[1] As JASP computes the slope parameter on zero-centered data in Bayesian Linear regression, it does not directly provide the intercept corresponding to the alternative model. Thus, to obtain the figure of the posterior regression model, the intercept was determined using the least-squares method implemented in Python (version 3.8.10). This involved fitting a regression line with the slope parameter, as determined by Bayesian linear regression in JASP, to the observed non-standardized data. This process yielded an intercept of 544.670. It should be noted that this intercept value, in the context of the Bayesian model comparison using Bayes factors, is not critical for model assessment, as the Bayes factor analysis is location-scale invariant (cf. Bernardo, 2007). This invariance implies that the model's comparison and inference remain consistent regardless of shifts or scaling in the predictor variable's values (cf. Bernardo, 2007).

posterior probability of the alternative model of 0.336, resulting in a BF10=0.505 and BF01=1.980, thus indicating that the observed data are 1.980 times more likely under the null model compared to the alternative model (cf. van den Bergh et al., 2021). Following interpretational conventions set by Jeffreys (1961), this data provides moderate evidence for the null model, but, due to the weakness of the evidence, is "not worth more than a bare mention" (Jeffreys, 1961, as cited in Taboga, 2021). In the context of the hypothesis under examination, this means that the analyzed data gives us no grounds for concluding that mean fronto-parietal theta coherence during a baseline video predicts latencies to orient towards a salient stimulus in a subsequent prediction task above the null level.

It should be noted that the Bayes factor favoring the null model does not indicate that the null model fits the data better than the alternative model. The mathematical structure of Bayes factor model selection inherently favors simpler models, thus embedding the principle of scientific parsimony in model selection (cf. La Rocca, 2013; Pericchi, 2005). Thus, a more complex model must justify its additional complexity by a significant (in a pre-theoretical, non-frequentist understanding) improvement in data fit. Thus, the obtained results indicate that the increase in data fit provided by the alternative model does not justify the introduction of the predictor mean fronto-parietal theta coherence into the model.

Figure 10

Distribution of Mean Latencies (Left) and Mean Coherence Values (Right)

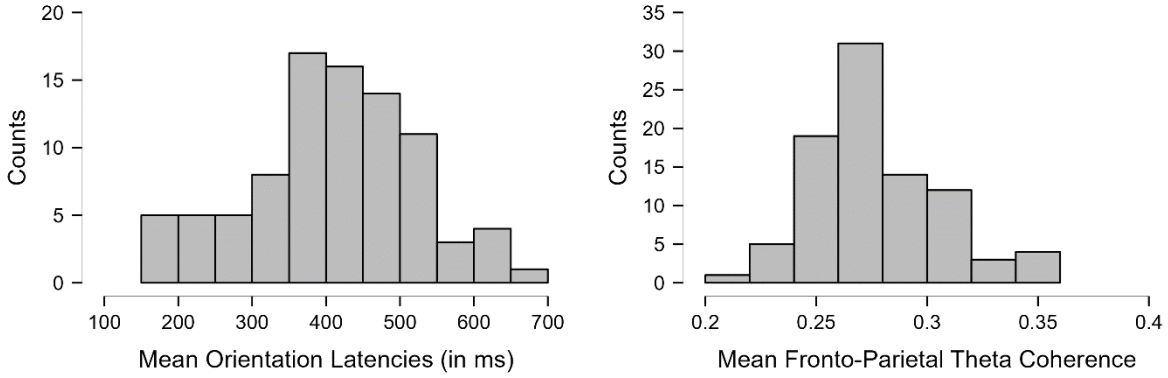

Figure 11

Posterior Distribution of Intercept (Left) and Covariate Mean Coherence (Right), Including 95% CI

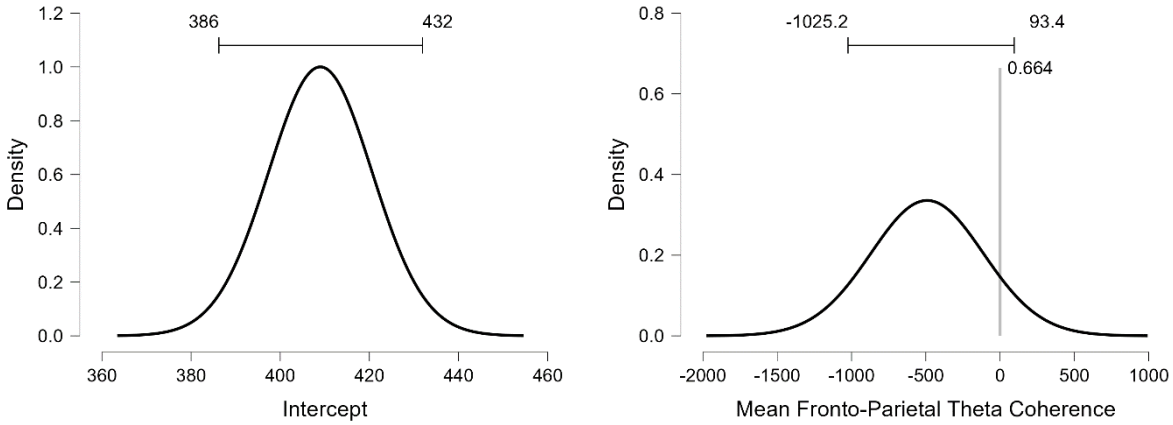

Figure 12

Scatterplot of Mean Orientation Latencies (in ms) Against Mean Fronto-Parietal Theta Coherence with Intercept Only Regression Line (Red) and its Credible Interval

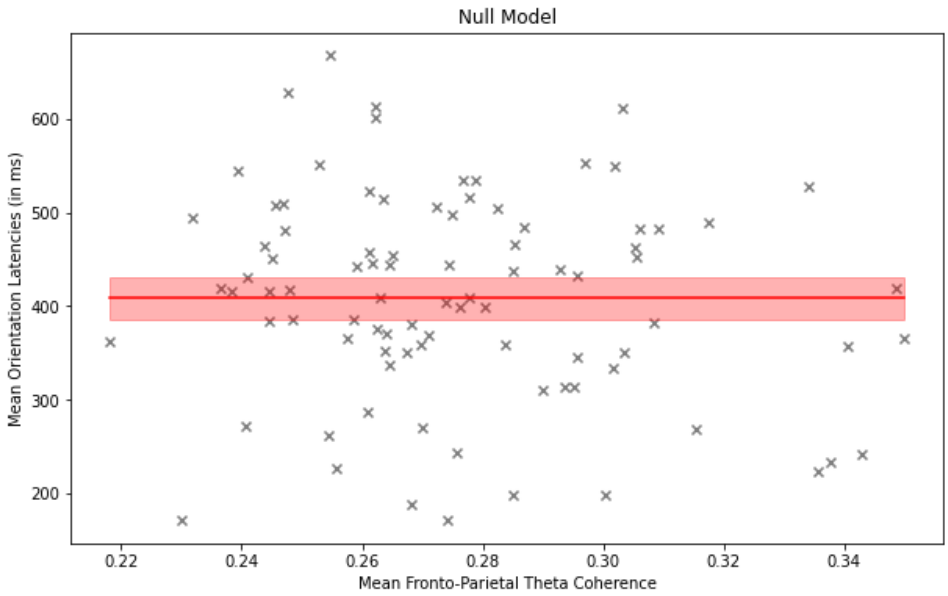

Figure 13

Scatterplot of Mean Orientation Latencies (in ms) Against Mean Fronto-Parietal Theta Coherence with Posterior Regression Line of the Alternative Model (Red) and its Credible Interval

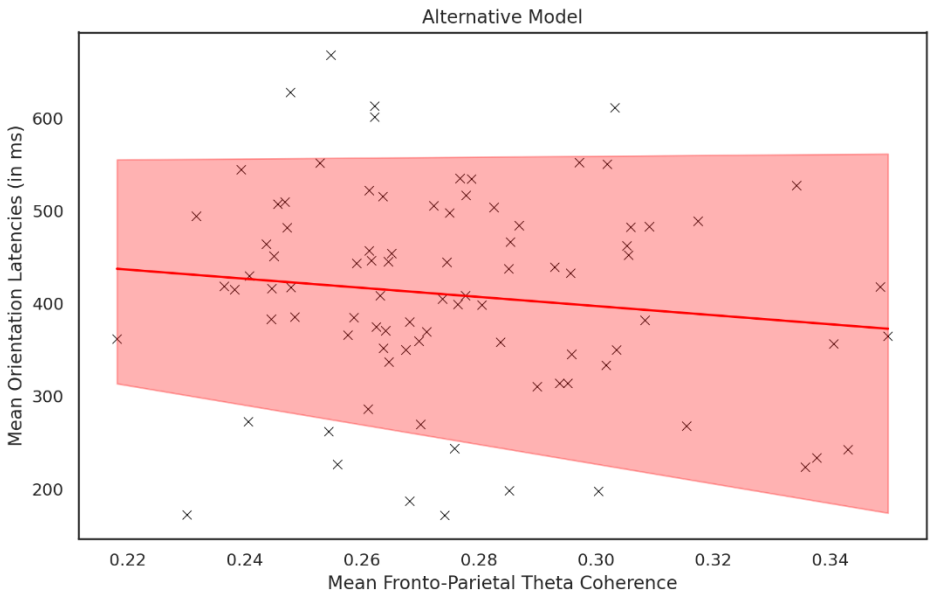

Discussion

The results of the present analysis do not indicate that mean orientation latencies during a baseline video predict mean latencies to orient in a subsequent prediction task. What are the implications of this finding for the hypothesis under examination, namely, that fronto-parietal theta synchronicity is a functional correlate of attention orienting and learning processes in infants?

A conservative interpretation of the results presented would imply reserving judgment given the notably low Bayes factor. In keeping with this perspective, more data and subsequent analyses are needed to reach a firmer and more definitive result in favor of either the null or the alternative model. This perspective aligns with the interpretive guidelines proposed by Jeffreys (1961), as referenced earlier.

Given the observed Bayes factor, making a binary decision (rejection or acceptance) would entail the acceptance of the null model, i.e., that there was no effect of theta coherence between frontal and parietal regions on orientation latencies in the task described. There could be different explanations for this:

The most straight-forward interpretation would be that the assumption of fronto-parietal theta coherence being a functional correlate of attention orientation and learning processes in six months old infants was inaccurate. Previous evidence based on infant studies gives us strong reasons to assume that theta power is associated with attention and learning processes in infants (Begus et al., 2015; Begus & Bonawitz, 2020; Orekhova et al., 1999; Orekhova et al., 2006; Xie et al., 2018). Furthermore, fronto-parietal theta synchronization has been reported to be a correlate of both top-down control and attention (Clayton et al., 2015; Cooper et al., 2015; Sauseng et al., 2005) and working memory (Sarnthein et al. 1998; Weiss et al., 2000) in adults and adolescents in various studies. One possible interpretation of the results of the present analysis in light of these previous reports is that although theta-power already plays a role in attention and learning processes in infants, efficient (i.e., task relevant) synchronization between frontal and posterior regions in the theta-band occurs only at a later age, thus explaining why no noteworthy effect of fronto-

parietal coherence on reduced orientation latencies was observed in the present study. Subsequent research could address this possibility by assessing whether the strength of fronto-parietal theta coherence changes as a function of infant age. Following this (somewhat speculative) interpretation, fronto-parietal theta synchronicity may constitute a marker of systemic neural maturation. It is also conceivable that, although theta-band synchronization between frontal and posterior regions already occurs at six months, it does not yet serve as a neural marker of attention and learning. This latter hypothesis could be addressed by subsequent research examining whether the predictive power of fronto-parietal coherence in an attention task increases with age. Last, it is possible that baseline fronto-parietal theta coherence is not a functional correlate of shortened orientation latencies, but that concurrent theta synchronization (i.e., synchronization during the task) is. The assumption underlying the present analysis was that baseline fronto-parietal coherence is a neural marker of stronger inter-area communication, and that this increased communication would influence performance during the task. However, it is conceivable that relevant synchronization only occurs during the task itself, so that there are no measurable differences during a baseline phase, hence rendering baseline measures inadequate as predictors of task performance. This hypothesis could be tested by conducting analyses similar to the one discussed in the present paper, but using concurrent coherence instead of baseline coherence as a predictor.

The different hypotheses just discussed assume that fronto-parietal theta-synchronicity during a baseline phase has no effect on orientation latencies in six months old infants in the described task. However, alternative interpretations of the presented findings make themselves available. Recognizing that scientific hypotheses cannot be tested in isolation but are assessed alongside various auxiliary hypotheses (Duhem, 1914/1954; Quine, 1951), another possibility is that while theta might play a role in attention and learning, it does not manifest in reduced latencies in the task employed in the current study. Put differently, the task might not have effectively captured individual differences in learning and attention processes. Thus, the root cause of the absence of a testable effect would be in

the manner of operationalization, rather than the true interaction of the underlying latent constructs.

Alternatively, the anticipated effect might have been present but overshadowed by data noise or other factors influencing reaction times, such as emotional states or fatigue. Given that the study was conducted on an infant population, this consideration appears reasonable, although it remains unverifiable with the available data. A noteworthy result in this context is the very wide credible interval of the posterior density function for the slope parameter of fronto-parietal theta coherence. This broad interval signifies substantial uncertainty about the effect's magnitude and crucially, its direction. While a straightforward interpretation of the Bayes factor might lean towards the null model, the expansive credible interval is compatible with the effects in both directions. Intriguingly, the 95% CI of the posterior density function is not symmetric around 0. Rather, it leans more heavily towards a negative than a positive deviation from 0, thus still almost reaching the lower bounds of medium-sized effect slopes (β= (-)0.30– (-)0.49, following Cohen, 1988) in the predicted direction. Thus, while the computed CI is compatible with the existence of a considerable effect in the anticipated direction, it is essential to underscore that no such effect emerged in this research. As alluded to earlier, the interval's width could be due to sample variability or external factors not considered in the research. This underlines the necessity of accumulating more data to decrease this uncertainty.

Considering the properties of the CI discussed and the guidelines for Bayes factor interpretation by Jeffreys (1961), it seems advisable to withhold judgment on the role of fronto-parietal theta coherence in infant attention and learning. The presented results neither confirm nor strongly refute this hypothesis, thus being compatible with but not providing evidence for a possible real-world effect.

To more precisely elucidate the role of theta coherence in infant cognition, future research should consider refining the methodologies used in the present study. Given the sensitivity of infant EEG to artifacts arising from movements, crying, and other disruptive behaviors, as well as a potential influence of emotional well-being on task performance in a

research population with less developed inhibitory control such as infants, future research may incorporate observational or physiological metrics to gauge emotional states and subsequently introduce them as model predictors. This would provide a more comprehensive analysis that accounts for variables that might confound or mediate the relationship between theta coherence and cognitive outcomes in infants. By taking such practical matters into account, the field could move closer to a clearer understanding of the intricate neural mechanisms at play in early cognitive development.

In summary, the aim of the present thesis was to examine a potential negative relation between fronto-parietal theta connectivity during a baseline task and the mean orientation latencies in a subsequent prediction task in 6-month-old infants. The basis for this prediction was the suspected functional role of fronto-parietal theta connectivity in attention and learning processes in infants, which – so the hypothesis – may positively correlate with the ability to learn environmental contingencies, which in turn should reduce measured orientation latencies. This hypothesis was tested using a Bayesian linear regression predicting mean orientation latencies on the basis of mean fronto-parietal theta band coherence. With a Bayes factor slightly favoring the null model, no such effect was observed in the current study, which may be taken to indicate that fronto-parietal theta coherence plays no role in learning and attention processes in infants, that functionally relevant fronto-parietal theta coupling has not yet emerged at six months, or that an existing effect was not adequately captured by the design and analysis used in the present thesis.

References

Addyman, C., & Mareschal, D. (2013). Local redundancy governs infants' spontaneous orienting to visual-temporal sequences. *Child development, 84*(4), 1137-1144. https://doi.org/10.1111/cdev.12060

Bastos, A. M., & Schoffelen, J. M. (2016). A tutorial review of functional connectivity analysis methods and their interpretational pitfalls. *Frontiers in systems neuroscience*, *9*. https://doi.org/10.3389/fnsys.2015.00175

Bear, M., Connors, B., & Paradiso, M. A. (2020). *Neuroscience: Exploring the Brain, Enhanced Fourth Edition*. Jones & Bartlett Learning.

Bechtel, W. (2008). *Mental Mechanisms: Philosophical Perspectives on Cognitive Neuroscience*. Routledge.

Begus, K., & Bonawitz, E. (2020). The rhythm of learning: Theta oscillations as an index of active learning in infancy. *Developmental Cognitive Neuroscience*, *45*(100810). https://doi.org/10.1016/j.dcn.2020.100810

Begus, K., Southgate, V., & Gliga, T. (2015). Neural mechanisms of infant learning: differences in frontal theta activity during object exploration modulate subsequent object recognition. *Biology Letters*, *11*(20150041). https://doi.org/10.1098/rsbl.2015.0041

Bell, M. A., & Wolfe, C. D. (2007). Changes in brain functioning from infancy to early childhood: Evidence from EEG power and coherence during working memory tasks. *Developmental Neuropsychology, 31*(1), 21-38. https://doi.org/10.1080/87565640709336885

Bendat, J. S., & Piersol, A. G. (1980). Engineering applications of correlation and spectral analysis. *New York*.

Bernardo, J. M. (2007). Objective Bayesian point and region estimation in location-scale models. *Statistics and Operations Research Transactions, 31*(1). Retrieved from http://hdl.handle.net/2099/3807

Bisina, K. V., & Azeez, M. A. (2017, June). Optimized estimation of power spectral density. In 2017 International Conference on Intelligent Computing and Control Systems (ICICCS) (pp. 871-875). Madurai, India. doi:10.1109/ICCONS.2017.8250588.

Bortel, R., & Sovka, P. (2006). EEG–EMG coherence enhancement. *Signal Processing*, *86*(7), 1737-1751. https://doi.org/10.1016/j.sigpro.2005.09.011

Bowyer, S.M. (2016). Coherence a measure of the brain networks: Past and present. *Neuropsychiatric Electrophysiology 2*(1) https://doi.org/10.1186/s40810-015-0015-7

Braithwaite, E. K., Jones, E. J., Johnson, M. H., & Holmboe, K. (2020). Dynamic modulation of frontal theta power predicts cognitive ability in infancy. *Developmental Cognitive Neuroscience*, *45*(100818). https://doi.org/10.1016/j.dcn.2020.100818

Bruns, A., & Eckhorn, R. (2004). Task-related coupling from high-to low-frequency signals among visual cortical areas in human subdural recordings. *International Journal of Psychophysiology, 51*(2), 97-116. https://doi.org/10.1016/j.ijpsycho.2003.07.001

Cavanagh, J. F., & Frank, M. J. (2014). Frontal theta as a mechanism for cognitive control. *Trends in Cognitive Sciences*, *18*(8), 414-421. https://doi.org/10.1016/j.tics.2014.04.012

Clayton, M. S., Yeung, N., & Kadosh, R. C. (2015). The roles of cortical oscillations in sustained attention. *Trends in Cognitive Sciences*, *19*(4), 188-195. https://doi.org/10.1016/j.tics.2015.02.004

Cohen, J. (1988). *Statistical Power Analysis for the Behavioral Sciences* (2nd ed.). Erlbaum.

Cohen, M. X. (2014). *Analyzing neural time series data: theory and practice*. MIT press.

Colgin, L. L. (2013). Mechanisms and functions of theta rhythms. *Annual Rreview of Neuroscience*, *36*, 295-312. https://doi.org/10.1146/annurev-neuro-062012-170330

Colombo, J. (2001). The development of visual attention in infancy. *Annual review of psychology*, *52*(1), 337-367. https://doi.org/10.1146/annurev.psych.52.1.337

Cooper, P. S., Wong, A. S., Fulham, W. R., Thienel, R., Mansfield, E., Michie, P. T., & Karayanidis, F. (2015). Theta frontoparietal connectivity associated with proactive

and reactive cognitive control processes. *Neuroimage*, *108*, 354-363. https://doi.org/10.1016/j.neuroimage.2014.12.028

Corbetta, M., & Shulman, G. L. (2002). Control of goal-directed and stimulus-driven attention in the brain. *Nature Reviews Neuroscience*, *3*(3), 201-215. https://doi.org/10.1038/nrn755

Craver, C., & Tabery, J. (2023). Mechanisms in Science. In E. N. Zalta & U. Nodelman (Eds.), *The Stanford Encyclopedia of Philosophy* (Fall 2023 Edition). Retrieved from https://plato.stanford.edu/archives/fall2023/entries/science-mechanisms/

Cuevas, K., & Bell, M. A. (2011). EEG and ECG from 5 to 10 months of age: Developmental changes in baseline activation and cognitive processing during a working memory task. *International Journal of Psychophysiology, 80(2)*, 119–128. https://doi.org/10.1016/j.ijpsycho.2011.02.009

de Vries, R. M., & Morey, R. D. (2013, March 4). Bayesian hypothesis testing for single-subject designs. Psychological Methods. Advance online publication. https://doi.org/10.1037/a003103

Delorme, A., & Makeig, S. (2004). EEGLAB: An open source toolbox for analysis of single-trial EEG dynamics including independent component analysis. *Journal of neuroscience methods, 134*(1), 9-21. https://doi.org/10.1016/j.jneumeth.2003.10.009

Duhamel, P., & Vetterli, M. (1990). Fast Fourier transforms: A tutorial review and a state of the art. Signal Processing, 19(4), 259-299. https://doi.org/10.1016/0165-1684(90)90158-U.

Duhem, P. (1954). *The Aim and Structure of Physical Theory* (P. P. Wiener, Trans.). Princeton University Press. (Original work published 1914)

Fingelkurts, A. A., Fingelkurts, A. A., & Kähkönen, S. (2005). Functional connectivity in the brain—is it an elusive concept?. *Neuroscience & Biobehavioral Reviews*, *28*(8), 827-836. https://doi.org/10.1016/j.neubiorev.2004.10.009

Franchak, J. M. (2020). Visual exploratory behavior and its development. *Psychology of Learning and Motivation, 73*, 59-94. https://doi.org/10.1016/bs.plm.2020.07.001

Friston, K. J. (1994). Functional and effective connectivity in neuroimaging: A synthesis. *Human Brain Mapping, 2*(1-2), 56-78. https://doi.org/10.1002/hbm.460020107

Friston, K. J., Frith, C. D., & Frackowiak, R. S. J. (1993a). Time-dependent changes in effective connectivity measured with PET. *Human Brain Mapping, 1*(1), 69-79. https://doi.org/10.1002/hbm.460010108

Friston, K. J., Frith, C. D., Liddle, P. F., & Frackowiak, R. S. (1993b). Functional connectivity: The principal-component analysis of large (PET) data sets. *Journal of Cerebral Blood Flow & Metabolism, 13*(1), 5-14. https://doi.org/10.1038/jcbfm.1993.4

Gou, Z., Choudhury, N., & Benasich, A. A. (2011). Resting frontal gamma power at 16, 24 and 36 months predicts individual differences in language and cognition at 4 and 5 years. *Behavioural Brain Research, 220*(2), 263–270. https://doi.org/10.1016/j.bbr.2011.01.048

Haartsen, R. (2019). EEG connectivity in infants at risk for autism spectrum disorder [Unpublished thesis]. ORBIT - Online Repository of Birkbeck Institutional Theses. https://eprints.bbk.ac.uk/id/eprint/40390/

Haith, M. M., Hazan, C., & Goodman, G. S. (1988). Expectation and anticipation of dynamic visual events by 3.5-month-old babies. *Child development 59*(2), 467-479. https://doi.org/10.2307/1130325

Heo, I., & Van de Schoot, R. (2020, November 6). Tutorial: Advanced Bayesian regression in JASP. Zenodo. https://doi.org/10.5281/zenodo.3991326

Hermens, D. F., Soei, E. X., Clarke, S. D., Kohn, M. R., Gordon, E., & Williams, L. M. (2005). Resting EEG theta activity predicts cognitive performance in attention-deficit hyperactivity disorder. *Pediatric Neurology*, *32*(4), 248-256. https://doi.org/10.1016/j.pediatrneurol.2004.11.009

James, W. (1981) *The Principles of Psychology*. Harvard University Press. (Original work published 1890)

JASP Team. (2023). *JASP* (Version 0.17.3) [Computer software]. https://jasp-stats.org/

Jeffreys, H. (1961). *Theory of Probability* (3rd ed.). Oxford University Press.

Johnson, M. H. (1990). Cortical maturation and the development of visual attention in early infancy. *Journal of Cognitive Neuroscience, 2*(2), 81-95. https://doi.org/10.1162/jocn.1990.2.2.81

Johnson, M. H., Posner, M. I., & Rothbart, M. K. (1991). Components of visual orienting in early infancy: Contingency learning, anticipatory looking, and disengaging. *Journal of Cognitive Neuroscience*, *3*(4), 335-344. https://doi.org/10.1162/jocn.1991.3.4.335

Jones, E. J., Goodwin, A., Orekhova, E., Charman, T., Dawson, G., Webb, S. J., & Johnson, M. H. (2020). Infant EEG theta modulation predicts childhood intelligence. *Scientific Reports*, *10*(11232). https://doi.org/10.1038/s41598-020-67687-y

Kidd, C., Piantadosi, S. T., & Aslin, R. N. (2012). The Goldilocks effect: Human infants allocate attention to visual sequences that are neither too simple nor too complex. *PloS one*, *7*(5), e36399. https://doi.org/10.1371/journal.pone.0036399

Kothe, C. A., & Makeig, S. (2013). BCILAB: A platform for brain-computer interface development. *Journal of Neural Engineering, 10*(5), 056014. https://doi.org/10.1088/1741-2560/10/5/056014

La Rocca, L. (2013). A comparison of objective Bayes factors for variable selection in linear regression models. In P. Giudici, S. Ingrassia, & M. Vichi (Eds.), *Statistical Models for Data Analysis (Studies in Classification, Data Analysis, and Knowledge Organization)*. Springer. https://doi.org/10.1007/978-3-319-00032-9_21

Lachaux, J. P., Rodriguez, E., Martinerie, J., & Varela, F. J. (1999). Measuring phase synchrony in brain signals. *Human brain mapping*, *8*(4), 194-208. https://doi.org/10.1002/(SICI)1097-0193(1999)8:4%3C194::AID-HBM4%3E3.0.CO;2-C

Lazar, M. (2010). Mapping brain anatomical connectivity using white matter tractography. *NMR in Biomedicine, 23*(7), 821-835. https://doi.org/10.1002/nbm.1579

Liebe, S., Hoerzer, G. M., Logothetis, N. K., & Rainer, G. (2012). Theta coupling between V4 and prefrontal cortex predicts visual short-term memory performance. *Nature Neuroscience*, *15*(3), 456-462. https://doi.org/10.1038/nn.3038

Lindner, A., Iyer, A., Kagan, I., & Andersen, R. A. (2010). Human posterior parietal cortex plans where to reach and what to avoid. *Journal of Neuroscience*, *30*(35), 11715-11725. https://doi.org/10.1523/JNEUROSCI.2849-09.2010

Lopez, K. L., Monachino, A. D., Morales, S., Leach, S. C., Bowers, M. E., & Gabard-Durnam, L. J. (2022). HAPPILEE: HAPPE in low electrode electroencephalography, a standardized pre-processing software for lower density recordings. *NeuroImage*, *260*, 119390. https://doi.org/10.1016/j.neuroimage.2022.119390

Lu, D., Ye, M., & Hill, M. C. (2012). Analysis of regression confidence intervals and Bayesian credible intervals for uncertainty quantification. *Water Resources Research, 48*(9). https://doi.org/10.1029/2011WR011289

MathWorks. (2023, November 6). *Magnitude-squared coherence - MATLAB mscohere*. https://www.mathworks.com/help/signal/ref/mscohere.html

Matsuzawa, M., & Shimojo, S. (1997). Infants' fast saccades in the gap paradigm and development of visual attention. *Infant Behavior and Development, 20*(4), 449-455. https://doi.org/10.1016/S0163-6383(97)90035-7

Meijer, E. J., Hermans, K. H. M., Zwanenburg, A., Jennekens, W., Niemarkt, H. J., Cluitmans, P. J. M., ... & Andriessen, P. (2014). Functional connectivity in preterm infants derived from EEG coherence analysis. *European journal of paediatric neurology*, *18*(6), 780-789. https://doi.org/10.1016/j.ejpn.2014.08.003

Miskovic, V., & Keil, A. (2015). Reliability of event-related EEG functional connectivity during visual entrainment: Magnitude squared coherence and phase synchrony estimates. *Psychophysiology*, *52*(1), 81-89. https://doi.org/10.1111/psyp.12287

Monachino, A. D., Lopez, K. L., Pierce, L. J., & Gabard-Durnam, L. J. (2022). The HAPPE plus Event-Related (HAPPE+ER) software: A standardized preprocessing pipeline for event-related potential analyses. *Developmental Cognitive Neuroscience, 57*, 101140. https://doi.org/10.1016/j.dcn.2022.101140

Monachino, A.D., Lopez, K.L., Pierce, L., & Gabard-Durnam, L. (2023). *HAPPE User Guide*. Pinelab. Retrieved from https://github.com/PINELab/HAPPE/blob/master/HAPPE%20User%20Guide.docx

Mountcastle, V. B. (1978). Brain mechanisms for directed attention. *Journal of the Royal Society of Medicine*, *71*(3), 14-28. https://doi.org/10.1177/014107687807100317

Mullen, T., 2012. *CleanLine EEGLAB Plugin*. [Computer Software] https://www.nitrc.org/projects/cleanline

Nelson, C. A., Thomas, K. M., & de Haan, M. D. (2012). *Neuroscience of cognitive development: The role of experience and the developing brain*. John Wiley & Sons.

Nolte, G., Bai, O., Wheaton, L., Mari, Z., Vorbach, S., & Hallett, M. (2004). Identifying true brain interaction from EEG data using the imaginary part of coherency. *Clinical Neurophysiology*, *115*(10), 2292-2307. https://doi.org/10.1016/j.clinph.2004.04.029

Nunez, P. L., & Srinivasan, R. (2006). *Electric fields of the brain: the neurophysics of EEG* (2nd ed.). Oxford University Press.

Nunez, P. L., Srinivasan, R., Westdorp, A. F., Wijesinghe, R. S., Tucker, D. M., Silberstein, R. B., & Cadusch, P. J. (1997). EEG coherency: I: statistics, reference electrode, volume conduction, Laplacians, cortical imaging, and interpretation at multiple scales. *Electroencephalography and Clinical Neurophysiology*, *103*(5), 499-515. https://doi.org/10.1016/S0013-4694(97)00066-7

Oppenheim, A. V., Willsky, A. S., Nawab, S. H., & Ding, J. J. (1997). *Signals and systems* (Vol. 2, pp. 74-102). Prentice hall.

Orekhova, E. V., Stroganova, T. A., & Posikera, I. N. (1999). Theta synchronization during sustained anticipatory attention in infants over the second half of the first year of life. *International Journal of Psychophysiology, 32*(2), 151-172. https://doi.org/10.1016/S0167-8760(99)00011-2

Orekhova, E. V., Stroganova, T. A., Posikera, I. N., & Elam, M. (2006). EEG theta rhythm in infants and preschool children. *Clinical Neurophysiology, 117*(5), 1047-1062. https://doi.org/10.1016/j.clinph.2005.12.027

Osipova, D., Takashima, A., Oostenveld, R., Fernández, G., Maris, E., & Jensen, O. (2006). Theta and gamma oscillations predict encoding and retrieval of declarative memory. *Journal of Neuroscience*, *26*(28), 7523-7531. https://doi.org/10.1523/JNEUROSCI.1948-06.2006

Pericchi, L.R. (2005). Model Selection and Hypothesis Testing based on Objective Probabilities and Bayes Factors. *Handbook of Statistics, 25,* 115-149. https://doi.org/10.1016/S0169-7161(05)25004-6

Perone, S., & Gartstein, M. A. (2019). Relations between dynamics of parent-infant interactions and baseline EEG functional connectivity. *Infant Behavior and Development, 57*, 101344. https://doi.org/10.1016/j.infbeh.2019.101344

Perone, S., Palanisamy, J., & Carlson, S. M. (2018). Age-related change in brain rhythms from early to middle childhood: Links to executive function. *Developmental Science, 21*(6), e12691. https://doi.org/10.1111/desc.12691.

Petersen, S. E., & Posner, M. I. (2012). The attention system of the human brain: 20 years after. *Annual review of neuroscience*, *35*, 73-89. https://doi.org/10.1146/annurev-neuro-062111-150525

Poli, F., Serino, G., Mars, R. B., & Hunnius, S. (2020). Infants tailor their attention to maximize learning. *Science Advances, 6*(39), eabb5053. https://doi.org/10.1126/sciadv.abb5053

Posner, M. I., & Petersen, S. E. (1990). The attention system of the human brain. *Annual Review of Neuroscience, 13*(1), 25-42. https://doi.org/10.1146/annurev.ne.13.030190.000325

Posner, M. I., & Rothbart, M. K. (2007). Research on attention networks as a model for the integration of psychological science. *Annual Review of Psychology, 58*, 1-23. https://doi.org/10.1146/annurev.psych.58.110405.085516

Posner, M. I., Petersen, S. E., Fox, P. T., & Raichle, M. E. (1988). Localization of cognitive operations in the human brain. *Science*, *240*(4859), 1627-1631. https://doi.org/10.1126/science.3289116

Puschner, P. (2010, October). Die Diskrete Fouriertransformation (DFT). Unpublished manuscript. Retrieved from https://ti.tuwien.ac.at/cps/teaching/courses/dspv/files/DFT-FFT.pdf

PyMC (2021a). *pymc.Cauchy*. PyMC 5.10.3 documentation. https://www.pymc.io/projects/docs/en/stable/api/distributions/generated/pymc.Cauchy.html

PyMC (2021b). *pymc.HalfCauchy*. PyMC 5.10.3 documentation. https://www.pymc.io/projects/docs/en/latest/api/distributions/generated/pymc.HalfCauchy.html

Quine, W. V. O. (1951). Two dogmas of empiricism. *The Philosophical Review, 60*(1), 20-43.

Rodriguez-Martinez, E. I., Barriga-Paulino, C. I., Rojas-Benjumea, M. A., & Gómez, C. M. (2013). Spontaneous theta rhythm and working memory co-variation during child development. *Neuroscience Letters*, *550*, 134-138. https://doi.org/10.1016/j.neulet.2013.06.054

Rouder, J. N., Speckman, P. L., Sun, D., Morey, R. D., & Iverson, G. (2009). Bayesian *t*-tests for accepting and rejecting the null hypothesis. *Psychonomic Bulletin & Review, 16*, 225-237. https://doi.org/10.3758/PBR.16.2.225

Ruess, J., Mattersberger, M., Brzozowska, A., Höhl, S. (2023, June 15). *Entrainment and its Influence on Looking Behaviour During Two Learning/Attention Tasks in Infants* [Poster presentation]. Early Career Researcher (ERC) Poster Event, Vienna, Austria.

Rutishauser, U., Ross, I. B., Mamelak, A. N., & Schuman, E. M. (2010). Human memory strength is predicted by theta-frequency phase-locking of single neurons. *Nature, 464*(7290), 903-907. https://doi.org/10.1038/nature08860

Sarnthein, J., Petsche, H., Rappelsberger, P., Shaw, G. L., & Von Stein, A. (1998). Synchronization between prefrontal and posterior association cortex during human working memory. *Proceedings of the National Academy of Sciences*, *95*(12), 7092-7096. https://doi.org/10.1073/pnas.95.12.7092

Sauseng, P., Klimesch, W., Schabus, M., & Doppelmayr, M. (2005). Fronto-parietal EEG coherence in theta and upper alpha reflect central executive functions of working memory. *International Journal of Psychophysiology*, *57*(2), 97-103. https://doi.org/10.1016/j.ijpsycho.2005.03.018

Schwartz, S., Kessler, R., Gaughan, T., & Buckley, A. W. (2017). Electroencephalogram coherence patterns in autism: An updated review. *Pediatric Neurology, 67*, 7-22. https://doi.org/10.1016/j.pediatrneurol.2016.10.018

Shaw, J. C. (1984). Correlation and coherence analysis of the EEG: a selective tutorial review. *International Journal of Psychophysiology*, *1*(3), 255-266. https://doi.org/10.1016/0167-8760(84)90045-X

Siegel, A. F. (2016). Multiple Regression: Predicting One Variable From Several Others. In *Practical Business Statistics* (Seventh Edition) (pp. 355-418). Academic Press. https://doi.org/10.1016/B978-0-12-804250-2.00012-2

Srinivasan, N. (2007). Cognitive neuroscience of creativity: EEG based approaches. *Methods*, 42(1), 109-116. https://doi.org/10.1016/j.ymeth.2006.12.008

Stahl, A. E., & Feigenson, L. (2015). Observing the unexpected enhances infants' learning and exploration. *Science*, *348*(6230), 91-94. https://doi.org/10.1126/science.aaa3799

Stam, C. J., Nolte, G., & Daffertshofer, A. (2007). Phase lag index: assessment of functional connectivity from multi channel EEG and MEG with diminished bias from common sources. *Human Brain Mapping*, *28*(11), 1178-1193. https://doi.org/10.1002/hbm.20346

Stephan, K. E., & Friston, K. J. (2009). Functional connectivity. In L. R. Squire (Ed.), *Encyclopedia of Neuroscience*. Elsevier. https://doi.org/10.5167/uzh-25725391-397

Stroganova, T. A., Orekhova, E. V., & Posikera, I. N. (1998). Externally and internally controlled attention in infants: an EEG study. *International Journal of Psychophysiology*, *30*(3), 339-351. https://doi.org/10.1016/S0167-8760(98)00026-9

Taboga, M. (2021). Jeffreys' scale. In *Lectures on Probability Theory and Mathematical Statistics* (Online appendix). Kindle Direct Publishing. https://www.statlect.com/fundamentals-of-statistics/Jeffreys-scale

Thompson, K. G., Biscoe, K. L., & Sato, T. R. (2005). Neuronal basis of covert spatial attention in the frontal eye field. *Journal of Neuroscience*, *25*(41), 9479-9487. https://doi.org/10.1523/JNEUROSCI.0741-05.2005

Tomalski, P., Moore, D. G., Ribeiro, H., Axelsson, E. L., Murphy, E., Karmiloff-Smith, A., … Kushnerenko, E. (2013). Socioeconomic status and functional brain development - associations in early infancy. *Developmental Science, 16*(5), 676–687. https://doi.org/10.1111/desc.12079.

van den Bergh, D., Clyde, M. A., Gupta, A. R. K. N., de Jong, T., Gronau, Q. F., Marsman, M., … & Wagenmakers, E. J. (2021). A tutorial on Bayesian multi-model linear regression with BAS and JASP. *Behavior Research Methods, 53*(6), 2351. https://doi.org/10.3758/s13428-021-01552-2

Vehtari, A., Gelman, A., & Gabry, J. (2017). Practical Bayesian model evaluation using leave-one-out cross-validation and WAIC. Statistics and Computing, 27(5), 1413–1432. https://doi.org/10.1007/s11222-016-9696-4

Vinck, M., Oostenveld, R., Van Wingerden, M., Battaglia, F., & Pennartz, C. M. (2011). An improved index of phase-synchronization for electrophysiological data in the presence of volume-conduction, noise and sample-size bias. *Neuroimage*, *55*(4), 1548-1565. https://doi.org/10.1016/j.neuroimage.2011.01.055

Von Stein, A., & Sarnthein, J. (2000). Different frequencies for different scales of cortical integration: from local gamma to long range alpha/theta synchronization. *International Journal of Psychophysiology*, *38*(3), 301-313. https://doi.org/10.1016/S0167-8760(00)00172-0

Weiss, S., Müller, H. M., & Rappelsberger, P. (2000). Theta synchronization predicts efficient memory encoding of concrete and abstract nouns. *NeuroReport*, *11*(11), 2357-2361.

Welch, P. D. (1967). The use of Fast Fourier Transform for the estimation of power spectra: A method based on time averaging over short, modified periodograms. *IEEE Transactions on Audio and Electroacoustics, AU-15*(2), 70–73. https://doi.org/10.1109/TAU.1967.1161901

Wöhrle, J. (2017, August 7). *Elektroenzephalografie (EEG)*. Springer Medizin. https://www.springermedizin.de/emedpedia/klinische-neurologie/elektroenzephalografie-eeg?epediaDoi=10.1007%2F978-3-662-44768-0_9

Wurtz, R. H., Goldberg, M. E., & Robinson, D. L. (1980). Arousal habituation selective attention eye movement vision monkey vigilance acquisition process perception. *Progress in Psychobiology and Physiological Psychology, 9*, 43–83.

Xie, W., Mallin, B. M., & Richards, J. E. (2018). Development of infant sustained attention and its relation to EEG oscillations: an EEG and cortical source analysis study. *Developmental Science, 21*(3), e12562. https://doi.org/10.1111/desc.12562

Yang, J., Rahardja, S., & Fränti, P. (2019). *Outlier detection: How to threshold outlier scores? In Proceedings of the International Conference on Artificial Intelligence, Information Processing and Cloud Computing* (Art. 37). 1-6. https://doi.org/10.1145/3371425.3371427

Zamora-López, G., Zhou, C., & Kurths, J. (2011). Exploring brain function from anatomical connectivity. *Frontiers in Neuroscience*, *23*(7), 821-35. https://doi.org/10.1002%2Fnbm.1579

Appendix I: Figures

Figure 6

Influence of Scaling Parameter r on Cauchy Distribution

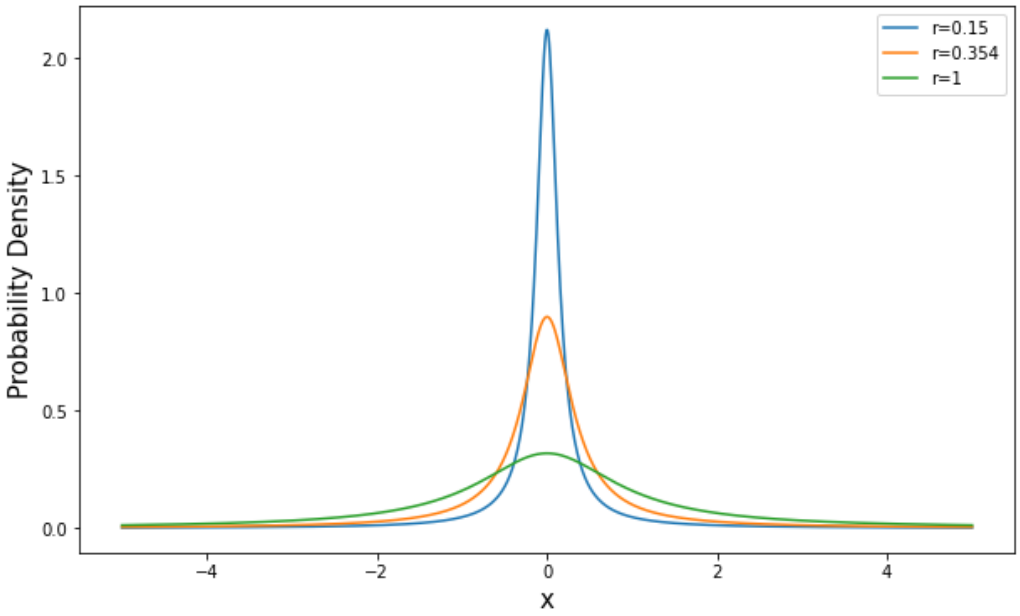

Figure 8

QQ-Plot

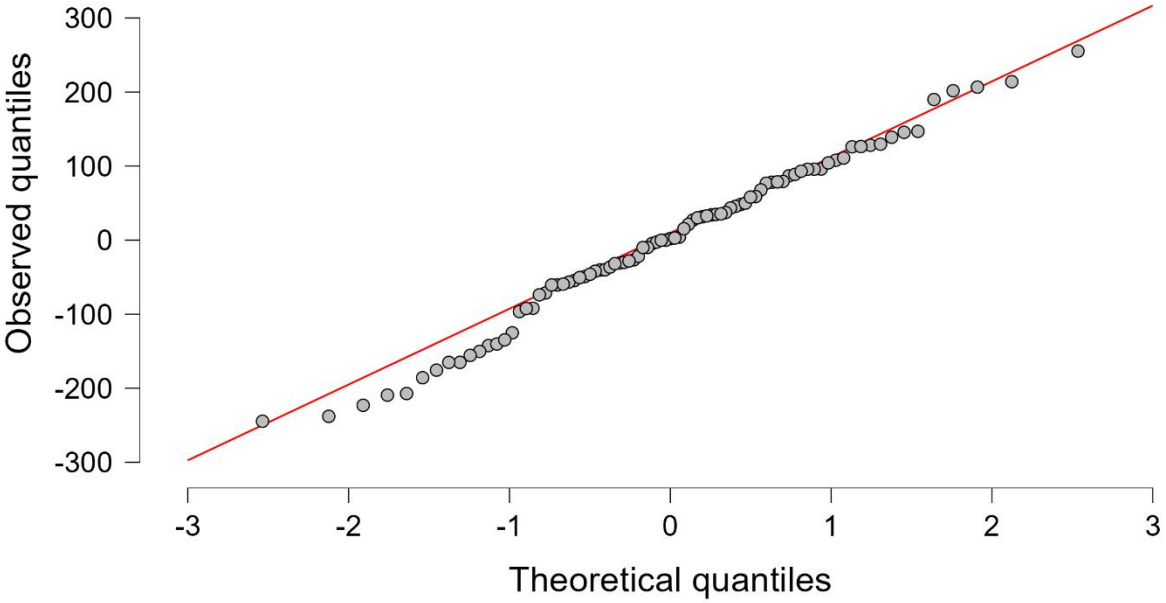

Figure 9

Residuals Plotted Against Model Predictions

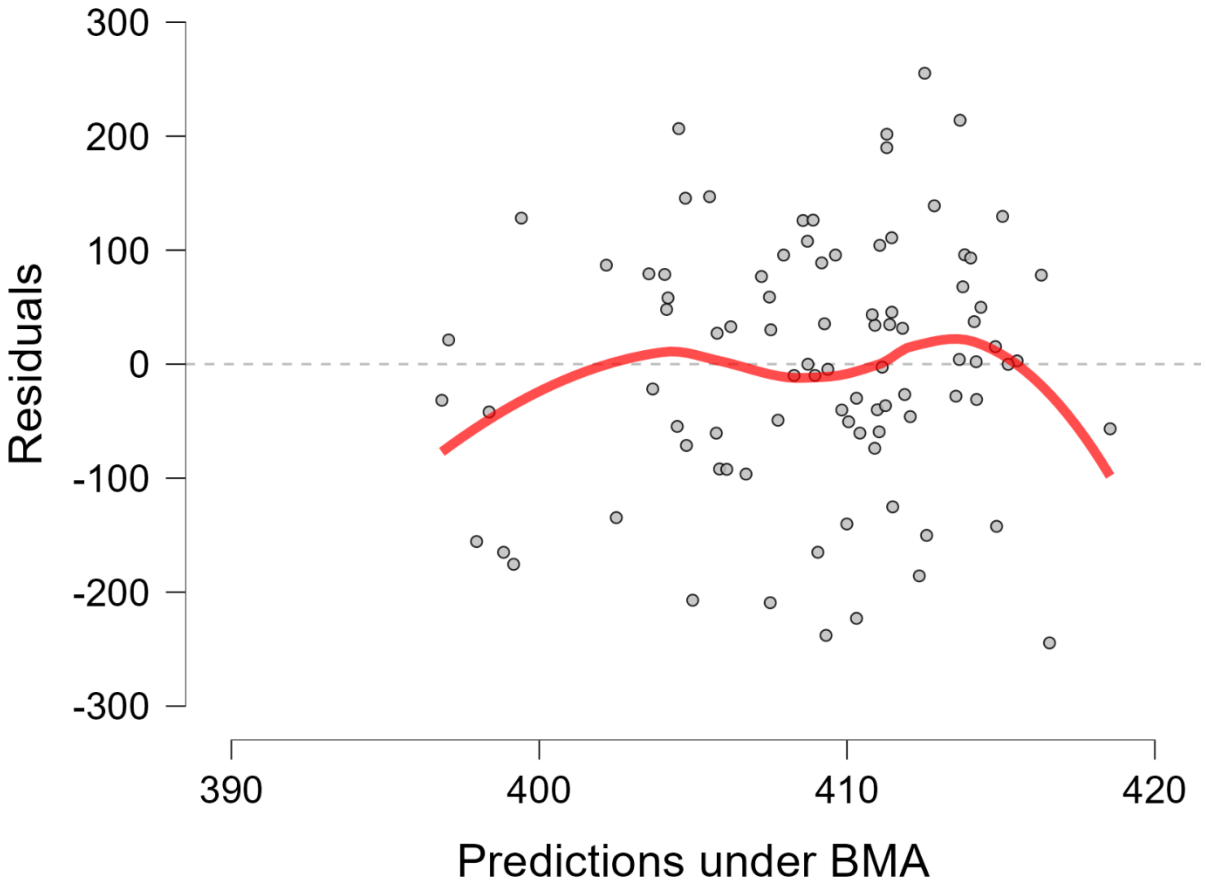

Appendix II: Analysis Scripts

Script Used in Section 'Orientation Latencies'

```
import numpy as np
import pandas as pd
#start = DI nr of first file to analyze; stop = DI nr of last
     file to analyze
#no need to keep python indexing (first included, last
     excluded) in mind, the code takes care of that
start = 1
stop = 140
def Latencies(DI):
    DI_nr = str(DI).zfill(3)
    path =
     'C:/Users/matte/Desktop/DynamIn_Video_csv/Raw_Data/DI{}.c
     sv'.format(DI_nr)
    #import the csv file
    df=pd.read_csv(path, delimiter=';', header=0,
     na_values=['N/A', 'NA'])
    #the try-except solution ensures that the code does not
     crash entirely when analysing many datafiles, but rather
     prints the DI-nr of the files
    #that do not work and continues with the others
    try:
        #duplicate the last row with a trigger and time stamps
     and rename the trigger to S1 (code won't run otherwise)
        # find the index of the last row containing 'R128'
```

```
   last_r128_idx = df.index[df['Response'] ==
'R128'].max()
   # create a new row with the same data as the previous
row
   new_row = df.iloc[last_r128_idx - 1].copy()
   # modify the Stimulus column to 'S 1'
   new_row['Stimulus'] = 'S  1'
   # insert the new row after the previous row
   df = pd.concat([df.iloc[:last_r128_idx],
new_row.to_frame().T, df.iloc[last_r128_idx:]])
   # reset the index
   df = df.reset_index(drop=True)
   #get rid of the unneccesarry columns (just for
aesthetic reasons)
   df.drop(columns=['Onset_Date', 'Offset_Date',
'Duration_Date'], inplace=True)
   #create an empty column for the onsets of the reward
stimuli
   df['Reward_Onset'] = np.nan
   #create a Boolean mask which picks out the S128
(photodiode reward onsets) which occur immediately after
the coded reward onsets
   mask = (df['Stimulus'] == 'S128') &
(df['Stimulus'].shift(1).isin(['S 40', 'S 41', 'S 42', 'S
43', 'S 44', 'S 45', 'S 46', 'S 47', 'S 48', 'S 49', 'S
74', 'S 75']))
```

```
   # apply the Bool. mask to set the values of
'Reward_Onset' to 'onset' for relevant S128s. This marks
the rows in the df in which the reward appears
   df.loc[mask, 'Reward_Onset'] = 'onset'
   #add the trial number to the df
   df['trial_number'] = (df['Reward_Onset'] ==
'onset').cumsum()
   #create a new column (empty) to mark the trials in
which the baby looks at the center when the reward
appears (=valid trials)
   df['Reward_Onset_valid'] = np.nan
   #To fill it...
   # iterate over each row in the dataframe
   for i, row in df.iterrows():
       # check if Reward_onset equals 'onset'
       if row['Reward_Onset'] == 'onset':
           # iterate over each row again to find a
matching 100 event
           for j, row2 in df.iterrows():
               # check if looking_behavior equals 100 and
the onset of the reward occurs during the central gaze
               if row2['looking_behavior'] == 100 and
row2['Onset_Time'] < row['Onset_Time'] <
row2['Offset_Time']:
                   # update the corresponding cell in the
Reward_onset_valid column to 'valid'
```

```
                    df.at[i, 'Reward_Onset_valid'] =
'valid'
                    break
   #create two empty columns for the direction of the
baby's gaze and the position of the reward (will be
filled later)
   df['gaze_direction'] = np.nan
   df['reward_position'] = np.nan
   #create an empty column which marks the trial type
(alpha, theta, mixed)
   df['trial_type'] = np.nan
   # create an empty column for the latencies
   df['latencies'] = float('nan')
       # loop through the rows of the dataframe
   for i, row in df.iterrows():
       # check if the current row contains a valid
stimulus event ('valid' = Baby looks a center during
reward onset)
       if row['Reward_Onset_valid'] == 'valid':
           # get the onset time of the valid stimulus
event
           stimulus_onset = row['Onset_Time']
           # find the corresponding event of the type 100
in the column "looking_behavior"
```

```
            event_100 = df.loc[(df['looking_behavior'] ==
100) & (df['Onset_Time'] <= stimulus_onset) &
(df['Offset_Time'] > stimulus_onset)]
            #define until when looking behavior can occur
for the latencies to still be calculated (current
version: S 1)
            trial_end = df.loc[(df['Stimulus'] == 'S  1')
& (df.index > i)].iloc[0]['Onset_Time']
            #The babies have time until the subsequent S 1
to look at the reward (the reward lingers a bit after the
"official" offset, this is to ensure we don't miss any
late looking behavior and thus bias our mean)
            # find the looking behavior of type 101 or 102
after the relevant central gaze
            event_after_100 =
df.loc[(df['looking_behavior'].isin([101, 102])) &
(df['Onset_Time'] >=
event_100['Offset_Time'].iloc[0])].iloc[0]
            # add the directions of the looking behavior
to the dataframe (not strictly necessary, but makes it
easier for me to work with the df)
            if event_after_100['looking_behavior'] == 101:
                df.loc[i, 'gaze_direction'] = 'left'
            elif event_after_100['looking_behavior'] ==
102:
                df.loc[i, 'gaze_direction'] = 'right'
```

```
            # enter the position of the reward depending
on the type of trial
            if df.loc[i-1, 'Stimulus'] in ['S 40', 'S 43',
'S 44', 'S 47', 'S 48', 'S 75']:
                df.loc[i, 'reward_position'] = 'left'
            elif df.loc[i-1, 'Stimulus'] in ['S 41', 'S
42', 'S 45', 'S 46', 'S 49', 'S 74']:
                df.loc[i, 'reward_position'] = 'right'
            # enter the trial type (theta, alpha, mixed)
to the frame
            if df.loc[i-1, 'Stimulus'] in ['S 40', 'S 41',
'S 42', 'S 43']:
                df.loc[i, 'trial_type'] = 'theta'
            elif df.loc[i-1, 'Stimulus'] in ['S 44', 'S
45', 'S 46', 'S 47']:
                df.loc[i, 'trial_type'] = 'alpha'
            elif df.loc[i-1, 'Stimulus'] in ['S 48', 'S
74']:
                df.loc[i, 'trial_type'] = 'mixed_theta'
            elif df.loc[i-1, 'Stimulus'] in ['S 49', 'S
75']:
                df.loc[i, 'trial_type'] = 'mixed_alpha'
            if df.loc[i, 'gaze_direction'] == df.loc[i,
'reward_position']:
```

```
                # check if the orientation behavior
 occurred within the relevant time period (i.e., while the
 stimulus is on display)
                if event_after_100['Onset_Time'] <
 trial_end:
                    # if so, calculate the orientation
 latencies by subtracting the onset of the reward from the
 onset of the orientation...
                    latency =
 (event_after_100['Onset_Time'] - stimulus_onset) * 1000
                    # ... and add the value to the
 dataframe
                    df.loc[i, 'latencies'] = latency
except:
    print("Error in:", DI)
#filter the latencies column to remove values lower than
 100ms
df['latencies'] = df['latencies'][df['latencies'] >= 100]
df = df.dropna(subset=['latencies'])
df = df.loc[:, ['trial_number', 'trial_type',
 'latencies']]
#calculate the mean latency of the participant if there
 were analyzable trials in the df
if df['latencies'].any():
    mean_latencies = np.mean(df['latencies'])
    print(DI, " has usable trials")
```

```
else:
    mean_latencies = np.nan
if df['latencies'].any():
    mean_latencies_theta = np.mean(df.loc[df['trial_type']
 == 'theta', 'latencies'])
    mean_latencies_alpha = np.mean(df.loc[df['trial_type']
 == 'alpha', 'latencies'])
    mean_latencies_mixed_alpha =
 np.mean(df.loc[(df['trial_type'] == 'mixed_alpha'),
 'latencies'])
    mean_latencies_mixed_theta =
 np.mean(df.loc[(df['trial_type'] == 'mixed_theta'),
 'latencies'])
count = df['latencies'].count()
theta_count = (df['trial_type'] == 'theta').sum()
alpha_count = (df['trial_type'] == 'alpha').sum()
mixed_alpha_count = (df['trial_type'] ==
 'mixed_alpha').sum()
mixed_theta_count = (df['trial_type'] ==
 'mixed_theta').sum()
mixed_count = mixed_alpha_count + mixed_theta_count
mean_latencies_mixed = np.mean(df.loc[((df['trial_type']
 == 'mixed_alpha') | (df['trial_type'] == 'mixed_theta')),
 'latencies'])
df.to_csv(path_or_buf=
 'C:/Users/matte/Desktop/DynamIn_Video_csv/Analyzed_Data/D
```

```
     I{}_with_latencies.csv'.format(DI_nr), sep = ';',
     index=False)
    #save the analyzed and updated file
    return mean_latencies, count, mean_latencies_theta,
     theta_count, mean_latencies_alpha, alpha_count,
     mean_latencies_mixed, mixed_count,
     mean_latencies_mixed_alpha, mixed_alpha_count,
     mean_latencies_mixed_theta, mixed_theta_count
df_lat = pd.DataFrame(columns=["DI_Nr", "Mean_Latencies",
     "n_of_valid_trials", "mean_latencies_theta",
     "theta_count", "mean_latencies_alpha", "alpha_count",
     "mean_latencies_mixed", "mixed_count"])
df_mixed_unformated = pd.DataFrame(columns=["DI_Nr",
     "mean_latencies_mixed_alpha", "mixed_alpha_count",
     "mean_latencies_mixed_theta", "mixed_theta_count"])
for i in range(start, stop+1):
    try:
        latencies, count, theta, theta_count, alpha,
     alpha_count, mixed, mixed_count,
     mean_latencies_mixed_alpha, mixed_alpha_count,
     mean_latencies_mixed_theta, mixed_theta_count  =
     Latencies(i)
        df_lat.loc[i] = [i, latencies, count, theta,
     theta_count, alpha, alpha_count, mixed, mixed_count]
    except:
        print(i, "is missing or has no valid trials")
```

```
print("n = ", df_lat.shape[0])

df_lat.to_csv(path_or_buf=

     'C:/Users/matte/Desktop/DynamIn_Video_csv/TEST_Mean_Laten

     cies_All_Trials.csv', sep = ';', index=False)
```

Input Parameters Used for HAPPILEE v.4 Preprocessing Pipeline

```
Density: Low (<= 30 channels)

Resting State or Task: Resting State

Data File Format: .set (EEGLab)

Acquisition Layout: Unspecified

Channels: All

Line Noise Frequency: 50 Hz

Line Noise Reduction Method: CleanLine - Default

Resample: Off

Filter:  - Lowpass Cutoff: 40

 - Highpass Cutoff: 1

 - Type: EEGLAB's FIR

Bad Channel Detection: On

 - Bad Channel Detection Order: Before Wavelet Thresholding

ECGone: Off

Wavelet Thresholding: Default

MuscIL: Off

Segmentation: On

 - Segment Length: 1 seconds

Interpolation: On

Segment Rejection: Off

Re-Referencing: On
```

```
 - Re-Reference Method: average
Visualizations: Off
Save Format: .set file
```

Script Used in Section 'Mean Coherence'

```
clear;
eeglab;
% Read the CSV file into a table
% Specify the full or relative path to the CSV file
csvFilePath = "C:\Users\matte\Desktop\EEG\4.
     EEG_PREPROCESSED_BASELINE\5 -
     quality_assessment_outputs\FINAL_INCLUSION\merged_inclusi
     on_FINAL.csv";
% Read the CSV file into a table
T = readtable(csvFilePath);
% Extract the numeric part using regular expressions
pattern = 'DI(\d+)_trimmed.set';
T.NumericPart = regexp(T.DI, pattern, 'tokens', 'once');
% Extract the numeric part cell array
filesCellArray = T.NumericPart;
% Convert the cell array of cell arrays to a cell array of
     strings
filesCellArray = cellfun(@(x) x{1}, filesCellArray,
     'UniformOutput', false);
% Convert the cell array of strings to a string array
filesStringArray = string(filesCellArray);
% Print the resulting string array
```

```
disp(filesStringArray);
start_file = "001";  % starting file
stop_file = "140";   % stopping file
output_csv_path =
     "C:\Users\matte\Desktop\EEG\BASELINE_COHERENCE.csv";
start = find(filesStringArray == start_file, 1);
stop = find(filesStringArray == stop_file, 1);
roi1_channels_names = {'F3', 'F4', 'Fz'};
roi2_channels_names = {'P3', 'P4', 'Pz'};
base_folder = "C:\Users\matte\Desktop\EEG\4.
     EEG_PREPROCESSED_BASELINE\4 - processed";
prefix = 'DI';
suffix = '_trimmed_processed';
file_format = '.set';
results_table = table([], [], 'VariableNames', {'FileName',
     'Mean_Coherence'});
for d = start:stop
    file_name = [prefix, filesStringArray{d}, suffix,
     file_format];
    full_path = fullfile(base_folder, file_name);
    if ~isfile(full_path)
        disp(['File not found: ', file_name]);
        continue;
    end
    EEG = pop_loadset('filename', char(full_path));
    disp(file_name);
```

```
roi1_channels_indices =
 find(ismember({EEG.chanlocs.labels},
 roi1_channels_names));
roi2_channels_indices =
 find(ismember({EEG.chanlocs.labels},
 roi2_channels_names));
% Get the latencies of the start of each epoch (assuming
 it's available in EEG.epoch.latency)
epoch_start_event_indices = [EEG.epoch(:).event];
epoch_start_latencies =
 [EEG.event(epoch_start_event_indices).latency];
look_codes = {'100', '101', '102'};
not_look_codes = {'99', '103', '104'};
is_valid_epoch = true(1, length(EEG.epoch));
is_looking_on_screen = true;
% Set the baseline epochs directly
baseline_start_epoch = 2;
baseline_end_epoch = 135;
for i = baseline_start_epoch:baseline_end_epoch
    current_epoch_event_types =
 {EEG.event(EEG.epoch(i).event).type};
   if any(ismember(current_epoch_event_types,
 not_look_codes))
        is_looking_on_screen = false;
        is_valid_epoch(i) = false;
    end
```

```
    if any(ismember(current_epoch_event_types,
 look_codes))
        is_looking_on_screen = true;
        is_valid_epoch(i) = false;
    end
    if ~is_looking_on_screen
        is_valid_epoch(i) = false;
    end
end
valid_epochs = find(is_valid_epoch);
% Display the number of valid epochs
disp(['Number of valid epochs: ',
 num2str(length(valid_epochs))]);
% Initialize a variable to store all mean coherences for
 the current file
all_mean_coherences = zeros(1, length(EEG.epoch));  %
 Initialize based on total epochs
coherence_idx = 1;  % Separate counter for storing
 coherences
for epoch_idx = valid_epochs
    segment_coherences = zeros(1,
 length(roi1_channels_indices) *
 length(roi2_channels_indices));  % Preallocated
    idx = 1;  % Counter for segment_coherences
    for ch1 = roi1_channels_indices
        for ch2 = roi2_channels_indices
```

```
            % Use mscohere for each channel pair within
 the valid epoch
            [Cxy, F] = mscohere(EEG.data(ch1,:,epoch_idx),
 EEG.data(ch2,:,epoch_idx), [], [], [], EEG.srate);
            theta_indices = (F >= 3) & (F <= 5);
            segment_coherences(idx) =
 mean(Cxy(theta_indices));
            idx = idx + 1;
        end
    end
    all_mean_coherences(coherence_idx) =
 mean(segment_coherences);  % Store coherence using the
 separate counter
    coherence_idx = coherence_idx + 1;
end
all_mean_coherences = all_mean_coherences(1:coherence_idx-
 1);  % Strip unused zeros
% Calculate the overall mean coherence for this
 participant
participant_mean_coherence = mean(all_mean_coherences);
disp(participant_mean_coherence)
% Load the existing CSV as a table
if isfile(output_csv_path)
    existing_data = readtable(output_csv_path);
else
```

```
        existing_data = table(); % If the file doesn't exist,
     start with an empty table
    end
    % Add the new results to the table
    new_entry = table({[prefix, filesStringArray{d}]},
     participant_mean_coherence, 'VariableNames', {'FileName',
     'MeanCoherence'});
    updated_data = [existing_data; new_entry];
    % Save the updated table back to the CSV
    writetable(updated_data, output_csv_path);
end
```

Script Used in Section 'Data Preparation & Exclusion Criteria'

```
import pandas as pd
import os
import numpy as np
from scipy import stats
import matplotlib.pyplot as plt
# Load the files into dataframes
df_mean_coherence =
     pd.read_csv("C:\\Users\\matte\\Desktop\\EEG\\BASELINE_COH
     ERENCE.csv")
df_mean_latencies =
     pd.read_csv("C:\\Users\\matte\\Desktop\\DynamIn_Video_csv
     \\Mean_Latencies_All_Trials.csv", sep = ';')
# Step 1: Convert and format the DI_number column
```

```
df_mean_latencies['DI_Nr'] =
     df_mean_latencies['DI_Nr'].astype(int) # Convert to
     integer
df_mean_latencies['FormattedDI'] =
     df_mean_latencies['DI_Nr'].apply(lambda x: 'DI' +
     str(x).zfill(3)) # Format to the desired structure
# Step 5: Merge the two dataframes
merged_df =
     df_mean_latencies.merge(df_mean_coherence[['FileName',
     'MeanCoherence']],
                                     left_on='FormattedDI',
                                     right_on='FileName',
                                     how='left')
# remove auxiliary columns
merged_df.drop(columns=['FormattedDI', 'FileName'],
     inplace=True)
merged_df.dropna(subset=['MeanCoherence'], inplace=True)
print(np.shape(merged_df))
def remove_outliers_iqr(data):
    Q1 = np.percentile(data, 25)
    Q3 = np.percentile(data, 75)
    IQR = Q3 - Q1
    lower_bound = Q1 - 1.5 * IQR
    upper_bound = Q3 + 1.5 * IQR
    # Create a mask to identify outliers
```

```
    outliers_mask = (data < lower_bound) | (data >
     upper_bound)
    return outliers_mask
# Create masks for 'MeanCoherence' and 'Mean_Latencies'
     columns
coherence_outliers =
     remove_outliers_iqr(merged_df['MeanCoherence'])
latencies_outliers =
     remove_outliers_iqr(merged_df['Mean_Latencies'])
# Combine the masks to identify participants who are outliers
     in either variable
participant_outliers = coherence_outliers | latencies_outliers
# Remove participants who are outliers in either variable
merged_df = merged_df[~participant_outliers]
print(np.shape(merged_df))
# Extract the directory path from the original path of
     df_mean_coherence
folder_path =
     os.path.dirname("C:\\Users\\matte\\Desktop\\EEG\\BASELINE
     _COHERENCE.csv")
# Construct the full path for the new file
save_path = os.path.join(folder_path,
     "Coherence_and_Latencies.csv")
# Save the dataframe to the specified path
merged_df.to_csv(save_path, index=False)
```

Script Used in Sections 'Statistical Analyses'/'Appendix III'

```
import pymc as pm
import arviz as az
import numpy as np
from scipy import stats,special
from matplotlib import pyplot as plt
import pandas as pd


from google.colab import files
files.upload()
Data=pd.read_csv('Coherence_and_Latencies.csv')


X_raw = np.array(Data['Mean Fronto-Parietal Theta
     Coherence'].values, dtype=np.float32)
Y1_raw = np.array(Data['Mean Orientation Latencies'].values,
     dtype=np.float32)
X = (X_raw - np.mean(X_raw)) / np.std(X_raw)
Y1 = (Y1_raw - np.mean(Y1_raw)) / np.std(Y1_raw)


with pm.Model() as Mod1:
    B0 = pm.Cauchy('B0', alpha=0, beta=0.354)
    B1 = pm.Cauchy('B1', alpha=0, beta=0.354)
    Err = pm.HalfCauchy('Err', beta=3)
    ll = pm.Normal('ll', mu= B0 + X * B1, sigma=Err,
     observed=Y1)
    trace = pm.sample(idata_kwargs={"log_likelihood": True})
```

```
with pm.Model() as Mod2:
  B0 = pm.Cauchy('B0', alpha=0, beta=0.354)
  B1 = pm.Cauchy('B1', alpha=0, beta=0.354)
  B2 = pm.Cauchy('B2', alpha=0, beta=0.354)
  Err = pm.HalfCauchy('Err', beta=3)
  ll=pm.Normal('ll',mu=B0 +[…]
     X*B1+(X**2)*B2,sigma=Err,observed=Y1)
  trace2=pm.sample(idata_kwargs={"log_likelihood": True})

with pm.Model() as Mod3:
  B0 = pm.Cauchy('B0', alpha=0, beta=0.354)
  B1 = pm.Cauchy('B1', alpha=0, beta=0.354)
  B2 = pm.Cauchy('B2', alpha=0, beta=0.354)
  B3 = pm.Cauchy('B3', alpha=0, beta=0.354)
  Err = pm.HalfCauchy('Err', beta=3)
ll=pm.Normal('ll',mu=B0+X*B1+(X**2)*B2+(X**3)*B3,sigma=Err,[…]
     observed=Y1)
  trace3=pm.sample(idata_kwargs={"log_likelihood": True})

print("Mod1", az.waic(trace))
print("Mod2", az.waic(trace2))
print("Mod3", az.waic(trace3))

CompareDict={}
CompareDict['Mod1']=trace
```

```
CompareDict['Mod2']=trace2

CompareDict['Mod3']=trace3

az.compare(CompareDict)
```

Appendix III: Nonlinear Models

To assess whether a non-linear model adequately captures the relation underlying the criterion (orientation latencies) – predictor (mean fronto-parietal theta coherence) relationship in the analyzed dataset, three increasingly more complex models were fitted and compared using Bayesian modelling in PyMC (version 5.7.2) and ArviZ (version 0.15.1). The model parameters β_0, β_1, β_2, and β_3 were defined using a Cauchy distribution with the location parameter alpha set to 0 and the scale parameter beta set to .356. More information about the properties of the Cauchy distribution as well as the reasoning behind using a scale parameter of .356 as the prior for the prediction parameters can be found in subsection 3.6. Note that the prior selection specified in said section only describes a prior choice for one parameter (scale parameter r) defining the slope, as JASP only allows for this parameter to be adjusted, whereas PYMC requires both the scale (named beta in PyMC) and the location parameter alpha (the mode of the distribution) of the distribution to be defined (PyMC, 2021a). The prior of the error term for all three models was defined as a Half-Cauchy distribution (consisting of the positive values of a Cauchy distribution with location parameter alpha = 0, cf. PyMC, 2021b) with beta set to 3. This prior choice makes for a very broad and unspecific prior, thus following the modelling choice explained in subsection 3.6 in the context of the JZS-prior for parameter distribution.

Using the thus defined priors, first, a simple linear regression model, consisting of a slope and an intercept parameter, as well as an error term, was fitted to the data. This model captures a linear relationship between the predictor and the outcome variable.

$$Y = \beta_0 + \beta_1 \times X + \epsilon$$

Second, a second-degree polynomial was fitted, which extends the linear model by adding a quadratic term.

$$Y = \beta_0 + \beta_1 \times X + \beta_2 \times X^2 + \epsilon$$

This model includes the intercept β_0, the linear term β_1, and an additional quadratic term β_2, and is designed to capture potential non-linear (quadratic) relationships between predictor and outcome. Last, a third-degree polynomial was fitted to the dataset, further extending the

previous model by a cubic term. This is the most complex model which was fitted and includes four parameters, β_0, β_1, β_2, and β_3, with β_3 capturing the cubic term, and is suitable for capturing more complex, cubic relationships between predictor and outcome.

$$Y = \beta_0 + \beta_1 \times X + \beta_2 \times X^2 + \beta_3 \times X^3 + \epsilon$$

Should a complex, non-linear relation (inverse u-shaped, s-shaped, etc.) hold between mean fronto-parietal theta coherence and orientation latencies, the more complex models would be able to adequately capture them, thus resulting in a superior model fit and out of sample predictive accuracy (cf. Vehtari et al., 2017). As described in section 3.6, this was not the case, with both WAIC and LOO values favoring the linear model (see section 3.6).

Appendix IV. Entrainment Analysis (ERC Poster): Entrainment and its Influence on Looking Behaviour During Two Learning/Attention Tasks in Infants

Background

Neural Entrainment: Neural entrainment describes the phase-alignment of brain oscillations to external periodic stimuli (de Graaf & Duecker, 2022). Numerous studies have shown the possibility of entraining the mature and developing brain with specific rhythms (Cantiani et al., 2022; Köster et al., 2019; Mathewson et al., 2012; Otero et al., 2022).

Theta Rhythms: Neural theta rhythms (between 3 -5 Hz in infants) seem to be associated with learning (Begus et al., 2015; Begus & Bonawitz, 2020) and sustained attention (Stroganova et al., 1998; Orekhova et al., 1999; Xie et al., 2018) in infants.

Alpha Rhythms: Neural alpha rhythms (between 5-9 Hz) seem to play a role in attention, perception, and memory (Klimesch, 1999; Tröndle et al., 2022; Xie et al., 2018). Contrary to the role of theta rhythms in attention, it has been observed that alpha waves are attenuated ('alpha desynchronization') in central and posterior regions during visual attention (Xie et al, 2018).

Gaze Cueing: Gaze cueing refers to shifting attention based on another person's gaze. It develops early in infancy and involves brain regions linked to social cognition (Mundy, 2018)

Current Study

This project aimed to investigate whether the frequency ("flickering rate") of presented stimuli influence infants' looking behavior in two attention/learning tasks. To do this, we analyzed the looking behavior of 6-month-old infants during a gaze cue and an ensuing prediction task. In both tasks, infants observed a face (central or lateral gaze) and two lateral stimuli flickering in different frequencies associated with either infants' alpha or theta brain oscillations. During the prediction task, the flickering rate of the stimuli predicted the spatial

orientation of a subsequent “reward” stimulus (moving cartoon character with sound).

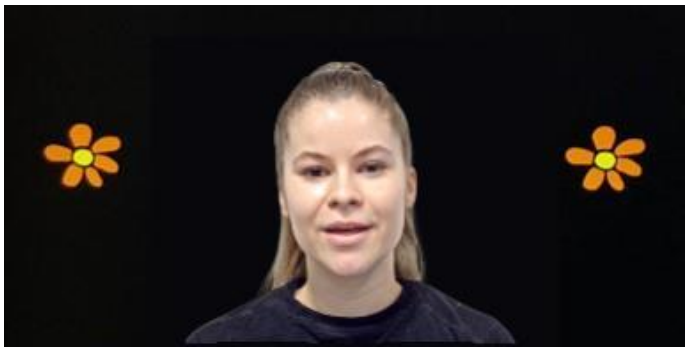

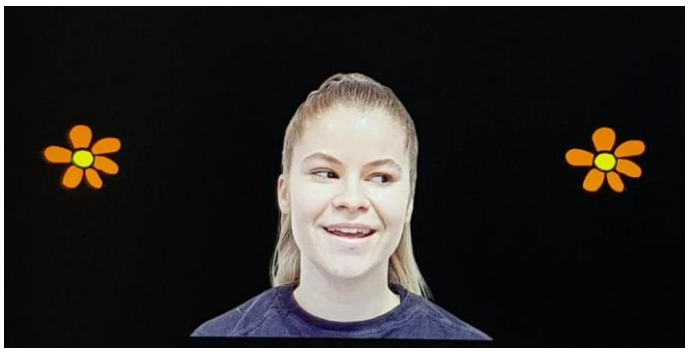

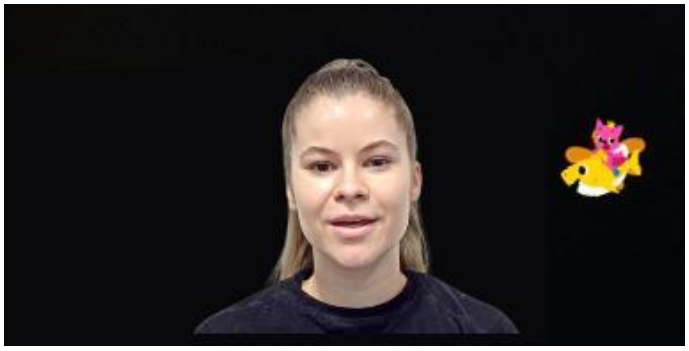

Our research questions were the following**:**

R1.1: Do infants follow the gaze cue in the gaze cue task and therefore spend more time oriented towards the gaze cued object than the gaze-averted object?

R1.2: Does the frequency of stimuli presentation set by the trial condition influence the infants‘ gaze following/ looking behavior?

R2: Is there a difference in orientation latencies towards the “reward” stimuli depending on the frequency (alpha or theta) of the predictive stimuli?

Analyses and Results

Gaze Cue Task

R1.1. Consistency in Gaze Following

We conducted a Wilcoxon signed-rank test (n = 128) in order to determine whether infants showed significantly more gaze cue consistent then gaze cue inconsistent looking behavior over all trial conditions.

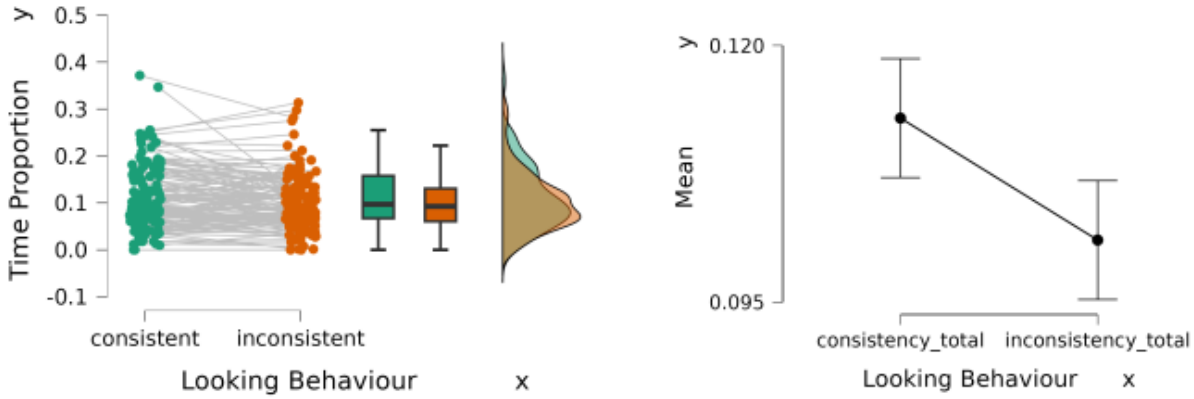

Results suggest that infants spent a significantly higher percentage of time looking at the gaze cued object (M = 0.113, SD = 0.07) then the gaze averted object (M = 0.101, SD = 0.06) ($p < .001$).

R1.2. Impact of Stimulus Frequency

We conducted a Bayesian Repeated Measures ANOVA (n = 128) to compare the infant's looking behavior between the three trial conditions: alpha (M = 0.114, SD = 0.08), theta (M = 0.116, SD = 0.08) and mixed (M = 0.116, SD = 0.09).

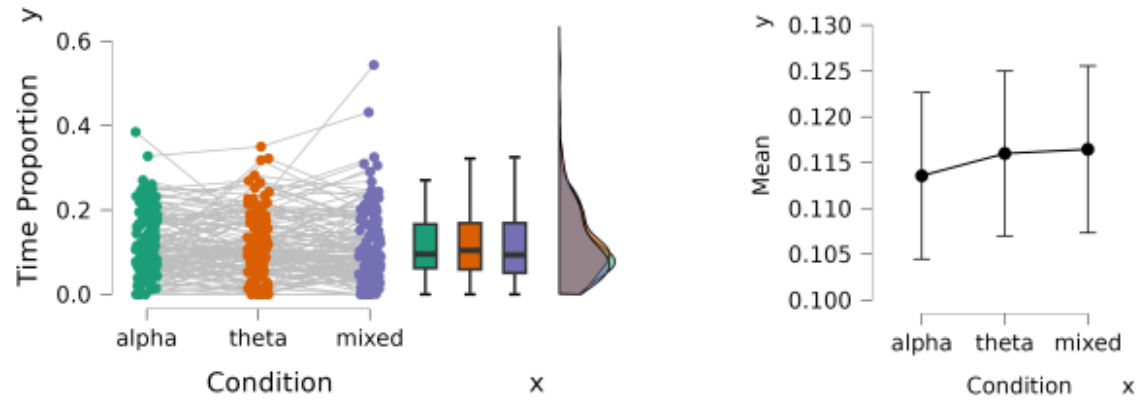

Our data suggests that infant looking behaviour was not influenced by the stimuli's frequency (BF01 = 30.968).

Prediction Task

R2. a) *All Trials*

We conducted a Bayesian Repeated Measures ANOVA (n = 63) to determine whether there was a difference between the mean latencies in the three trial types (alpha, theta, mixed). The evidence strongly suggests that there is no such difference (BF_{01} = 14.607)

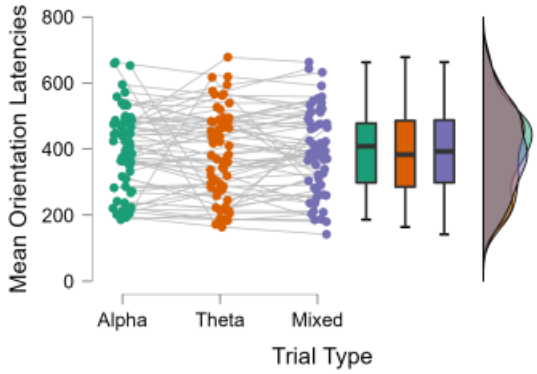

Descriptives

Trial Type	Mean	SD	N	95% Credible Interval Lower	95% Credible Interval Upper
Alpha	396.89	125.22	63	365.36	428.43
Theta	388.53	131.33	63	355.46	421.61
Mixed	393.58	125.81	63	361.89	425.26

b) Mixed Trials

A Bayesian Independent Means t-Test (n=63) was conducted to assess whether the predictive frequency (alpha or theta) influenced orientation latencies in Mixed Trials. No such effect was found, though the evidence is less conclusive in this analysis (BF01 = 3.156)

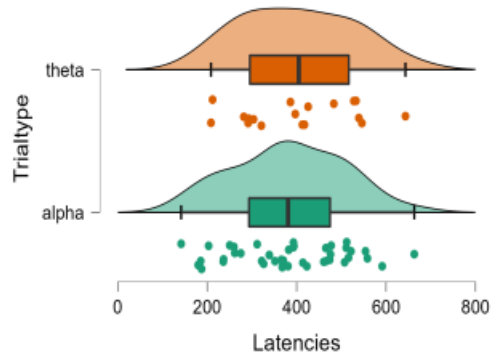

Descriptives

Group	N	Mean	SD	95% Credible Interval Lower	95% Credible Interval Upper
alpha	43	382.51	123.65	344.46	420.56
theta	18	401.36	125.24	339.08	463.64

Conclusions

Infants' Gaze Following Ability at 6-Months of Age

In line with existing literature on gaze following in infants, our results showed that 6-month old infants spent a significantly higher proportion of time during the trials looking at the caze cued object than the gaze-averted object. The frequency of object presentation did not have any influence on the gaze following behavior in our sample.

Influence of Frequency on Orientation Latencies

We found no systematic influence of stimulus flickering frequencies on latencies to orient. As neural entrainment was not assessed in the current analysis, it remains open whether the observed absence of an effect is due to a lack of entrainment to the stimulus rhythms or due to entrainment occurring but not resulting in an effect on orientation latencies.

References

Begus, K., & Bonawitz, E. (2020). The rhythm of learning: Theta oscillations as an index of active learning in infancy. *Developmental Cognitive Neuroscience*, *45*, 100810. https://doi.org/10.1016/j.dcn.2020.100810

Begus, K., Southgate, V., & Gliga, T. (2015). Neural mechanisms of infant learning: differences in frontal theta activity during object exploration modulate subsequent object recognition. *Biology Letters*, *11*(20150041). https://doi.org/10.1098/rsbl.2015.0041

Cantiani, C., Dondena, C., Molteni, M., Riva, V., & Piazza, C. (2022). Synchronizing with the rhythm: Infant neural entrainment to complex musical and speech stimuli. *Frontiers in Psychology*, *13*, 944670. https://doi.org/10.3389/fpsyg.2022.944670

de Graaf, T. A., & Duecker, F. (2022). No effects of rhythmic visual stimulation on target discrimination: An online alpha entrainment experiment. *European Journal of Neuroscience*, *55*(11–12), 3340–3351. https://doi.org/10.1111/ejn.15483

Klimesch, W. (1999). EEG alpha and theta oscillations reflect cognitive and memory performance: A review and analysis. *Brain Research Reviews*, *29*(2–3), 169–195. https://doi.org/10.1016/S0165-0173(98)00056-3

Köster, M., Langeloh, M., & Hoehl, S. (2019). Visually Entrained Theta Oscillations Increase for Unexpected Events in the Infant Brain. *Psychological Science*, *30*(11), 1656–1663. https://doi.org/10.1177/0956797619876260

Mathewson, K. E., Prudhomme, C., Fabiani, M., Beck, D. M., Lleras, A., & Gratton, G. (2012). Making Waves in the Stream of Consciousness: Entraining Oscillations in EEG Alpha

and Fluctuations in Visual Awareness with Rhythmic Visual Stimulation. *Journal of Cognitive Neuroscience*, *24*(12), 2321–2333. https://doi.org/10.1162/jocn_a_00288

Mundy, P. (2018). A review of joint attention and social-cognitive brain systems in typical development and autism spectrum disorder. *European Journal of Neuroscience*, *47*(6), 497–514. https://doi.org/10.1111/ejn.13720

Orekhova, E. V., Stroganova, T. A., & Posikera, I. N. (1999). Theta synchronization during sustained anticipatory attention in infants over the second half of the first year of life. *International Journal of Psychophysiology: Official Journal of the International Organization of Psychophysiology*, *32*(2), 151–172. https://doi.org/10.1016/s0167-8760(99)00011-2

Otero, M., Lea-Carnall, C., Prado, P., Escobar, M.-J., & El-Deredy, W. (2022). Modelling neural entrainment and its persistence: Influence of frequency of stimulation and phase at the stimulus offset. *Biomedical Physics & Engineering Express*, *8*(4), 045014. https://doi.org/10.1088/2057-1976/ac605a

Stroganova, T. A., Orekhova, E. V., & Posikera, I. N. (1998). Externally and internally controlled attention in infants: an EEG study. *International Journal of Psychophysiology*, *30*(3), 339-351. https://doi.org/10.1016/S0167-8760(98)00026-9

Tröndle, M., Popov, T., Dziemian, S., & Langer, N. (2022). Decomposing the role of alpha oscillations during brain maturation. *ELife*, *11*, e77571. https://doi.org/10.7554/eLife.77571

Xie, W., Mallin, B. M., & Richards, J. E. (2018). Development of infant sustained attention and its relation to EEG oscillations: An EEG and cortical source analysis study. *Developmental Science*, *21*(3), e12562. https://doi.org/10.1111/desc.12562